



Universiteit  
Leiden  
The Netherlands

## **Unearthing the past without a trowel: A comparative study on remote sensing techniques at Voulokaliva site 1990/35, Halos, Greece (Late Neolithic to the Early Iron Age)**

Kuiters, Aaricia

### **Citation**

Kuiters, A. (2022). *Unearthing the past without a trowel:: A comparative study on remote sensing techniques at Voulokaliva site 1990/35, Halos, Greece (Late Neolithic to the Early Iron Age)*.

Version: Not Applicable (or Unknown)

License: [License to inclusion and publication of a Bachelor or Master thesis in the Leiden University Student Repository](#)

Downloaded from: <https://hdl.handle.net/1887/3454598>

**Note:** To cite this publication please use the final published version (if applicable).

## Unearthing the past without a trowel:

A comparative study on remote sensing techniques at Voulokaliva site 1990/35,  
Halos, Greece (Late Neolithic to the Early Iron Age)



Aaricia Kuiters (s2211882)

Figure front page: Overview of Voulokaliva site 1990/35 created with the optical data collected by Jitte Waagen in November 2021

Unearthing the past without a trowel,

A comparative study on remote sensing techniques at Voulokaliva site 1990/35, Halos,  
Greece (Late Neolithic to the Early Iron Age)

Aaricia Kuiters

S2211882

BA3 thesis

Supervisor: Dr. T. Kalayci, Ph.D.

Digital archaeology

The University of Leiden, Faculty of Archaeology

Leiden, June 2022, Final version

## Acknowledgments

First and foremost, I would like to thank my supervisor, Tuna Kalayci, for his guidance in finding this exciting research topic and his clear feedback throughout writing this thesis. My thesis would have been impossible without the data and information he provided. Also, I would like to acknowledge Jitte Waagen, Vladimir Stissi and Apostolos Sarris, who collected and presented the remote sensing data of Voulokaliva site 1990/35.

In addition, I would like to thank my friends for supporting me throughout my study and helping me out during stressful times. You helped me maintain my passion for archaeology and provided me with four fantastic university years.

I appreciate everyone that I encountered during my four years of studying archaeology at the faculty of Leiden. Thank you for the interesting lectures, discussions and assignments that helped me advance within the field of archaeology.

Finally, I would like to express my gratitude to my family, who gave me my love for nature, adventure and history. They taught me to follow my passion and they have always encouraged my enthusiasm for archaeology. Also, I would like to thank my partner for his patience and continuous support. This thesis could not have been realized without their unconditional love and words of encouragement.

# Contents

Acknowledgments.....	4
1. Introduction.....	7
1.1 Introduction and problem statement .....	7
1.2 Objectives .....	8
1.3 Research questions.....	8
1.4 Methods and approach .....	9
1.5 Thesis outline.....	9
2. Voulokaliva site 1990/35.....	11
2.1 Environment, climate and soil conditions.....	11
2.2 Archaeological background .....	13
2.3 Concluding remarks.....	15
3. Theoretical Framework .....	16
3.1 Electromagnetic theory.....	16
3.2 Aerial imagery.....	17
3.2.1 Thermography .....	18
3.2.2 Multi-Spectral Imagery.....	20
3.3 Geophysical prospection .....	22
3.3.1 Ground Penetrating Radar .....	22
3.3.2 Geomagnetic Survey.....	23
3.3.3 Electromagnetic Induction Survey .....	25
3.3.4 Earth Resistance Survey .....	26
3.4 Concluding remarks.....	28
4. Methodology and approach.....	29
4.1 Materials.....	29
4.2 Methodology .....	30
4.3 A comparative approach to remote sensing techniques .....	32

5.	Results .....	33
5.1	Results of the remote sensing data.....	33
5.1.1	Thermography .....	33
5.1.2	Multi-Spectral Imagery .....	34
5.1.3	Ground Penetrating Radar .....	37
5.1.4	Geomagnetic Survey.....	38
5.1.5	Electromagnetic Induction Survey .....	38
5.1.6	Earth Resistance Survey .....	39
5.2	Results of the comparative approach .....	40
5.3	Concluding remarks.....	43
6.	Discussion .....	44
6.1	Reflecting on the results.....	44
6.1.1	Aerial imagery.....	44
6.1.2	Geophysical prospection .....	46
6.1.3	Comparative analysis.....	47
6.2	Interpretation of the results.....	47
6.3	Concluding remarks.....	50
7.	Conclusion .....	51
7.1	Introduction.....	51
7.2	Future research .....	52
	Abstract .....	54
	Bibliography.....	55
	List of figures .....	59
	List of tables .....	60
	List of appendices.....	61
	Appendix I.....	62
	Appendix II.....	65

# 1. Introduction

## 1.1 Introduction and problem statement

Remote sensing techniques are widely applied within the archaeological field and have a long history of scientific research (Tapete, 2018). According to Campana (2016), a possible definition of remote sensing is the science of examining materials without physical contact. This definition would exclude ground-based geophysical prospection since several geophysical instruments make contact with the ground. This thesis applies another definition put forward by Campana (2016), in which remote sensing involves every non-destructive technique applied to discover buried archaeological remains or study natural features. The non-destructive nature of these techniques opens up the possibility to explore archaeological sites before, during and after excavations or surveys. Remote sensing can be applied at a micro- and macro-level scale to identify potential archaeological sites, features and relics (Themistocleous et al., 2013). The capability of these techniques to discover archaeological remains in diverse environments is established by the large variety of literature on the subject (Sarris et al., 2013).

However, the rapidly evolving application of remote sensing techniques calls for a better understanding of the relationship between the technique and the visibility of archaeological anomalies. The influence of external factors on remote sensing data has been highlighted by numerous scientific studies (Agudo et al., 2018; Armstrong & Kalayci, 2015; Casana et al., 2017; Manataki et al., 2015; Schmidt, 2013). Remote sensing data is susceptible to variables such as environmental conditions, soil matrix, vegetation and moisture content. These external factors determine which anomalies appear on the data and which remain undetectable. However, not every remote sensing application is sensitive to each variable and detected anomalies can vary significantly between datasets.

Consequently, the latest trend in scientific research is focused on integrating remote sensing data since a single technique might not uncover all types of archaeological features (Agapiou & Lysandrou, 2015; Simon et al., 2015). An assessment of the different techniques and their theoretical background is necessary to explain why certain anomalies appear on specific datasets. This information can be used in applied and targeted research at potential archaeological sites. For instance, when a site has very distinct soil and weather conditions, remote sensing techniques that respond well to these circumstances can be applied and poor results due to external factors can be reduced.

This thesis aims at constructing a framework of various remote sensing techniques to assess their potential in detecting archaeological anomalies under specific circumstances. This framework is



applied in a case study located at Voulokaliva site 1990/35 in Thessaly, Greece. Voulokaliva site 1990/35 has been subjected to several archaeological prospection techniques, including fieldwalking survey, aerial imagery and geophysical prospection. The large number of applied techniques facilitates a comparative analysis. This comparative approach is used to determine which remote sensing techniques prove the most effective at Voulokaliva site 1990/35 and how this relates to their theoretical background. A better understanding of the theory behind remote sensing techniques, the influence of external variables and their relation to each other can significantly improve the detection of archaeological remains. This thesis' objectives are discussed in more detail in the following section.

## 1.2 Objectives

This thesis aims to discuss the possibilities and limitations of remote sensing techniques applied in archaeology. This research's theoretical ambition is to construct a consolidated overview of different remote sensing techniques, their applicability in archaeological prospection, and the ideal conditions to collect their respective datasets. This thesis takes a comparative approach to examine which techniques provide the best results in visualizing archaeological remains, which is investigated by means of a case study at Voulokaliva site 1990/35 (hereafter referred to as "Voulokaliva"). The main objective is to gain a better understanding of why certain remote sensing applications provide the best results. A theoretical framework is used to outline the possibilities and limitations of different techniques, which is then applied to the results of Voulokaliva. This research will support future remote sensing operators in deciding which technique should be employed when dealing with specific environmental circumstances, comparable to Voulokaliva.

## 1.3 Research questions

The research objectives are investigated by a number of research questions. The following main question is proposed.

How do the different remote sensing techniques operate in visualizing potential archaeological remains at Voulokaliva site 1990/35, Halos, Greece (Late Neolithic to the Early Iron Age) and how can these findings aid in developing a more targeted approach to archaeological prospection?

The sub-questions, as follows, aid in answering the main question.

- What are the ideal conditions to collect data with six respective remote sensing technologies, namely thermography, multi-spectral imagery, ground penetrating radar, geomagnetic survey, electromagnetic induction survey and earth resistance survey, and how can this knowledge be applied in archaeological prospection?
- Which anomalies can be detected on the remote sensing imagery and how do they compare?
- How do the detected anomalies relate to the theoretical background of the applied remote sensing techniques?
- To what extent do the anomalies correspond to the hypotheses based on previously executed field survey campaigns?
- Which remote sensing techniques prove the most effective in visualizing archaeological remains at Voulokaliva site 1990/35?

These sub-questions will be touched upon in chapter 3, 5 and 6. Chapter 7 combines the sub-questions to discuss and answer the main question. The following section elaborates on the methods used to answer the proposed research questions.

#### 1.4 Methods and approach

This thesis will use a comparative analysis of remote sensing techniques to assess the potential of both aerial imagery and geophysical prospection at Voulokaliva.

The thermal and multi-spectral data is visualized and analyzed in the open-source software QGIS. The data is visually scanned for anomalies that might indicate archaeological features, which are collected in a vector dataset. Sarris has analyzed the geophysical data since great expertise on the subject is necessary for an accurate interpretation (Sarris et al., 2016).

The thermal, multi-spectral and geophysical anomalies are compared. Anomalies that appear on multiple datasets are highlighted as well as irregularities that only appear on one dataset. Extensive literature research on the theoretical framework of each technique will be performed to examine why certain anomalies appear on specific datasets. Multiple factors will be taken into account, such as weather conditions, climate, soil conditions and the nature of the archaeological features.

The comparative analysis of the extensive remote sensing dataset collected at Voulokaliva will provide a framework to define the ideal conditions for archaeological prospection in the Mediterranean.

#### 1.5 Thesis outline

Chapter 2 introduces Voulokaliva by discussing its environmental and archaeological background.

The available data at this site has provided a framework for the theory and methodology behind this

research. An in-depth assessment of the remote sensing techniques applied at Voulokaliva will be presented in chapter 3. The theory behind each technique, as well as its archaeological potential, are discussed. The methodology and materials applied in this research are introduced in chapter 4. The materials consist of fieldwalking survey data and the data from six remote sensing techniques, specifically thermography, multi-spectral imagery, ground-penetrating radar, geomagnetic survey, electromagnetic induction survey and earth resistance survey. The remote sensing data is combined in a QGIS file, where they are subjected to varying analysis and data enhancement techniques. After the data preparation, a comparative approach is applied to assess the potential of remote sensing data at Voulokaliva. With the theory of chapter 3 and the background information on Voulokaliva in mind, the different datasets are visually scanned for archaeological anomalies. The results are summarized in chapter 5 and integrated into a comparative analysis. Chapter 6 will provide a critical review of the materials used, the interpretation of the data and the accuracy of the results. The conclusions are framed by the research questions and results and are outlined in chapter 7. This thesis concludes with potential areas of future research to enhance the integration of archaeological remote sensing techniques.

## 2. Voulokaliva site 1990/35

This chapter introduces the case study at Voulokaliva by discussing the environment, climate and soil conditions as well as the archaeological background. This information is essential in discovering and interpreting potential archaeological remains on remote sensing data. The environmental and soil conditions can shed light on why certain anomalies appear on the datasets, whereas others remain unexposed. The archaeological background of the region provides insights into the expected archaeology and is used to guide the interpretation of the detected anomalies.

### 2.1 Environment, climate and soil conditions

Voulokaliva is located at the Almiros and Sourpi Plains in Thessaly, Greece and measures approximately 18,500 m<sup>2</sup>. The Almiros and Sourpi plains were formed during the Tertiary and Quaternary and consist of a neo-tectonic basin defined by Alpine structures (Floras & Sgouras, 2004). According to Floras and Sgouras (2004), the Voulokaliva area involves a slightly sloping region in which the geology consists of Quaternary loose, mixed sediments. These sediments developed from the leaching and erosion of older formations and range from clayey silts to sands, gravels or grits. The deposits show a high rate of leaching and erosion and medium to high permeability (Floras & Sgouras, 2004). Voulokaliva is situated near the national highway and the River Amprysos. The area is marked and cut in half by a dirt road. In 2021 Waagen and colleagues collected drone data at Voulokaliva, during which they measured the soil and weather conditions. Appendix I contains all information collected during these drone flights. The superficial layer involves a sandy clay soil and the soil matrix mainly consists of clay (J. Waagen, personal communication, the 11th of April, 2022).

According to Loukas and colleagues (2008), this part of Thessaly has a Mediterranean climate indicated by hot and dry summers and cold and wet winters. The area shows significant temperature differences between the summer and the winter and the mean annual precipitation is approximately 700 mm. Loukas et al. (2008) discuss periods of extreme drought in Thessaly from the mid-1970s onwards. The significantly reduced amount of rainfall has impacted agriculture and natural vegetation in the area (Loukas et al., 2008).

The Voulokaliva area is marked by dense agricultural activities and natural vegetation. Sentinel-2 satellite data acquired at the Copernicus Open Access Hub from the European Space Agency indicates the phenological crop cycle in the Voulokaliva region (Congedo, 2021). Figure 1 shows that in April 2021, the vegetation was very dense, whereas in August 2021, the area contained almost no vegetation. November 2021, on the other hand, shows much variation in vegetation coverage. The weather conditions collected by Waagen and his team show that in August 2021 the moisture conditions were dry with a relative humidity of 32.5 at its lowest and 52.2 at its highest. The

temperatures varied between 27.0 °C and 34.9 °C. In November there was some occasional rainfall and a relative humidity of 55.0 at its lowest and 80.0 at its highest. The temperatures varied between 12.6 °C and 16.8 °C (J. Waagen, personal communication, the 11th of April, 2022). The geophysical data was collected on the 15<sup>th</sup> of April 2015, which according to Weather Underground (<https://wunderground.com>) was a dry day with temperatures ranging from 8 °C at night to 20 °C during the day. Light rain had occurred a week before, but no significant rainfall is documented.

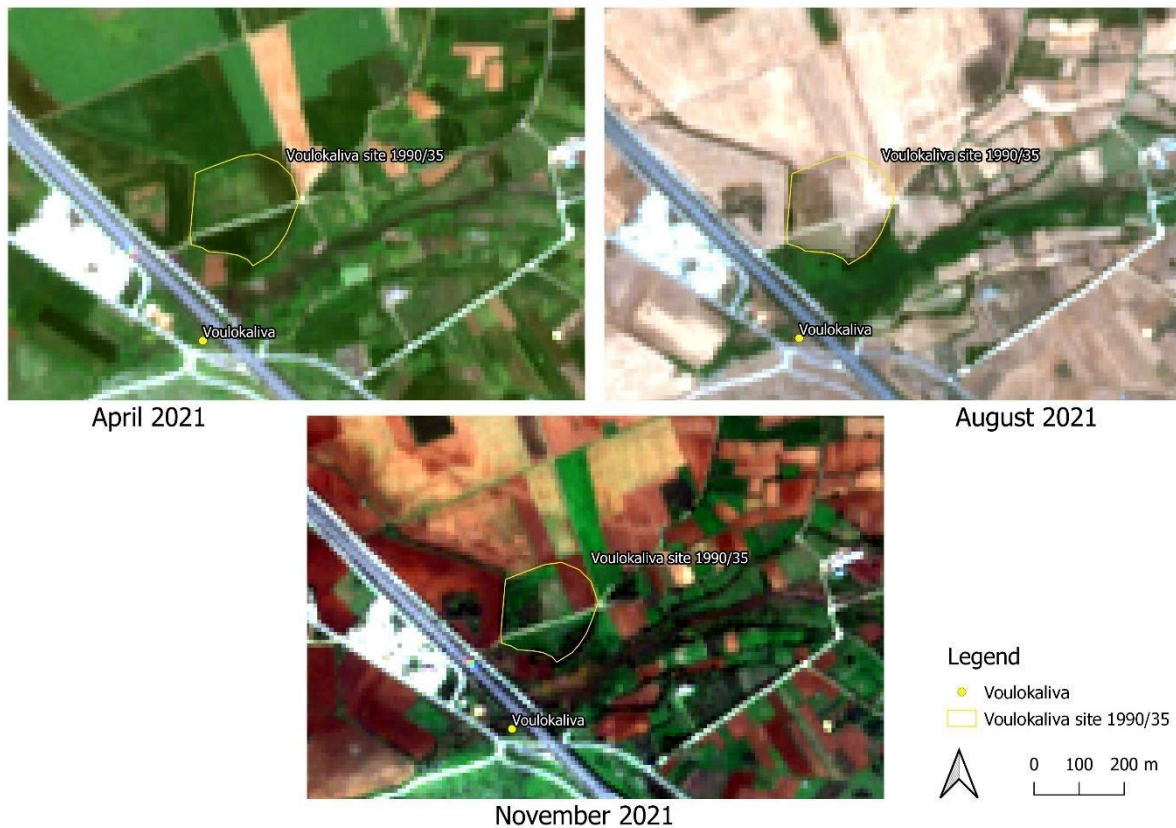


*Figure 1. Sentinel-2 RGB data of Voulokaliva site 1990/35 in April, August and November 2021*

The modern site of Voulokaliva can be divided into four vegetation regions. The northwestern region is filled with olive trees, whereas the north-eastern, south-eastern and southwestern areas consist of agricultural crops, mainly wheat. The agricultural areas show differentiation in the phenological crop cycle, which might be related to the type of cultivated crop. Some parts of the research area also contain patches of clover and the south-eastern region is partly covered by different trees (J. Waagen, personal communication, the 11th of April, 2022).

The following section will present the archaeological background of Voulokaliva site 1990/35.

## 2.2 Archaeological background

According to Karouzou (2019), Thessaly has a rich occupation history, which can be explained by the fertile plains and abundance of resources. The fertile soil provided sufficient agricultural produce and the conditions were ideal for keeping horses and livestock, while the surrounding mountains and Lake Karla provided timber, fish and game. During prehistoric times, Thessalian settlements were often placed on magoules, which involve low hills often close to water sources (Karouzou, 2019). Voulokaliva can be found in the vicinity of the ancient city of Halos. Halos comprised one of the earliest fieldwork campaigns in Greece led by Dutch archaeologists and research is conducted to this day. Extensive field surveys have yielded a considerable number of finds in the area, which demonstrates the archaeological potential of this region (Stissi et al., 2015).

Voulokaliva shares its name with the nearby Early Iron Age tumulus cemetery. Of all tumuli discovered at the cemetery, only tumulus 36 was partly published by Lagia and colleagues (2013). They state that mound 36 was continuously used and provides essential insights into mortuary practices during the Early Iron Age in Thessaly. The Voulokaliva tumulus shows elaborate practices that indicate a complex relationship with the deceased. The mound contained human and animal cremation remains, offering tables, fired ceramics and metals, funerary feasts and the removal or secondary disposal of remains (Lagia et al., 2013). Voulokaliva is hypothesized to be connected with the tumulus cemetery, but the actual function remains unknown. In 1990 field survey campaigns were set up to discover the chronology and activities at site 1990/35.

From 2011 to 2013, Stissi and his team (2015) revisited the site and resurveyed the area. They picked up over 7000 finds, of which 4000 belonged to the Final Neolithic period until the Middle Bronze Age, with the majority dating from the Early Bronze Age and corresponding to the first habitation period. One hundred sixty-five sherds date to the Late Bronze Age, 381 to the Early Iron Age and 308 sherds belong to either one of the periods. Also, more than 1000 fragments of tiles were dated to the Middle Ages or Early Modern Age. Besides sherds, many chipped stone artifacts and ground stone tools were collected. An important discovery was the chronological division of the fields. Finds dating from the Late Neolithic until the Early Bronze Age are mainly located in the northern plot (1266), whereas finds dating from the Late Bronze Age are clustered in plot 1269 in the southwestern part of the site. This suggests possible chronological differentiation within the area. Also, the Early Iron Age finds can be divided into two classes. The finds in field 1266 date up to the Archaic and are younger than the materials in fields 1268 and 1269, which mainly belong to the Protogeometric Period (figure 2). The first group is hypothesized to have belonged to the Voulokaliva tumulus cemetery. The Protogeometric finds, on the other hand, indicate a continuation of the Late Bronze Age (Christmann & Karimali, 2004; Stissi, 2004; Stissi et al., 2015).



*Figure 2. Map of the fieldwalking survey in 2011-2013 depicting the find collection grids and field numbers by Jitte Waagen (Stissi et al., 2015)*

Stissi et al. (2004) provide three possible interpretations of Voulokaliva site 1990/35. The first idea is that the site contained a sacred place connected with the nearby burial mounds. However, the site was abandoned before the funeral landscape had gone out of use, which is unusual since sanctuaries were often used for a long period of time. Another possibility would be that Voulokaliva was a burial site. There are no visible remains of burial mounds or stones at the surface and the only option would be inhumation in a small number of graves or cemetery. However, the most likely hypothesis is that Voulokaliva was an occupational site. This is substantiated by the strategic location of the site and close vicinity to the funerary landscape (Stissi et al., 2004). According to Karouzou (2019), Thessalian settlements during the Late Bronze Age and Early Iron Age were located close to water resources, important land passes or roads, controlled large amounts of arable lands and were often placed on low hills or magoules. Comparable settlement sites in Thessaly dating from the Late Bronze Age and Early Iron Age have uncovered structural remains with stone socles and mud-brick superstructures. If indeed Voulokaliva was a settlement, the expected features could contain remnants of roads, stone and mud-brick walls and other structural remains (Karouzou, 2019). Reinders (2004) highlights that the Late Neolithic and Early Bronze Age settlements are often indicated by pits and ditches, whereas the Late Bronze Age and Early Iron Age show an increase in structural remains.

The large size and chronological span of Voulokaliva make this site a crucial part in the understanding of the Voulokaliva area from the Late Neolithic onwards. The funerary landscape of the area is thoroughly investigated, but relatively little is known about the occupational and other remains. A

better understanding of Voulokaliva might shed light on the activities and function of this region. The large number of finds dating from the Late Neolithic and Early Bronze Age indicate a significant settlement. In contrast, the lack of finds dating from the Middle Bronze Age demonstrates a gap in the continuation of the site. The low number of Late Bronze Age finds suggest the presence of a settlement, which extended into the Protogeometric Period (Christmann & Karimali, 2004; Stissi, 2004; Stissi et al., 2004, 2015). However, Karouzou (2019) states that if this site were related to habitation during the Late Bronze Age, it would have been no more than a small village. This is supported by Sarris and colleagues (2016), who argue that local, handmade artifacts and an absence of imported items indicate an independent community sustained by the River Amprysos.

In April 2015, Sarris and colleagues carried out a geophysical survey at Voulokaliva. The results of this survey are summarized in the technical report and will be discussed in the subsequent chapters (Sarris et al., 2016). In August and November 2021, the site was visited by Waagen and colleagues who applied aerial imagery to collect thermal, optical and multi-spectral data. This thesis aims at analyzing and interpreting these datasets. The comparative analysis is focused on both the geophysical survey and the aerial imagery data.

### 2.3 Concluding remarks

The large number of prospection techniques applied at Voulokaliva, make it a suitable location for comparative analysis. Field survey results have highlighted the archaeological potential of the region and can be used in the interpretation of the remote sensing results. The distinct Mediterranean climate and recorded weather and soil conditions during aerial imagery acquisition by Waagen and his team provide the information needed for a theoretical assessment of the remote sensing results. The theoretical framework introduced in the following chapter and site conditions will be employed to explain the anomalies discovered on the different datasets.



### 3. Theoretical Framework

This section expands on the theory behind the remote sensing data. For organizational purposes, remote sensing is divided into aerial imagery and geophysical prospection. This thesis will use the definition put forward by Sarris (Sarris, 2017), who stated that geophysical prospection is ground-based and collected at the Earth's surface. In contrast, aerial imagery is collected by Remotely Piloted Aircraft Systems (RPASs), also known as drones. Chapter 3 aims at answering the following research question:

- What are the ideal conditions to collect data with six respective remote sensing technologies, namely thermography, multi-spectral imagery, ground penetrating radar, geomagnetic survey, electromagnetic induction survey and earth resistance survey, and how can this knowledge be applied in archaeological prospection?

#### 3.1 Electromagnetic theory

Remote sensing techniques often rely on the relationship between electromagnetic energy and the object under investigation (Jensen, 2014). A basic understanding of electromagnetic theory is necessary to interpret remote sensing data. Electromagnetic radiation is a wave-like phenomenon, which is created by a moving magnetic field and a moving electric field. The fields oscillate and produce an electromagnetic wave that travels through space with the speed of light (approximately  $3 \times 10^8 \text{ m s}^{-1}$ ). However, when electromagnetic energy interacts with matter, it gains particle-like characteristics. The wave-particle duality is a key concept within quantum mechanics (Jensen, 2014; Verhoeven, 2017). For this thesis the interaction between electromagnetic energy and objects is the most significant. The process consists of three steps:

1. A source (e.g., the sun) emits electromagnetic radiation. This radiation is measured in spectral irradiance  $E(\lambda)$ . The object partially reflects, transmits and absorbs the radiation.
2. The spectral irradiance  $E(\lambda)$  and unique reflectance of the object  $R(\lambda)$  form the spectral radiance  $L(\lambda)$  [i.e.,  $L(\lambda) = E(\lambda) \times R(\lambda)$ ], which is captured by the imaging sensor.
3. After the spectral sensitivity imager captures the spectral radiance, it is registered into spectral regions. Every pixel is denoted as many values as spectral bands in the imaging device (Verhoeven, 2017).

The amount of electromagnetic energy reflected, transmitted or absorbed depends on the physical, chemical and biological characteristics of the object (Jensen, 2014). Part of the self-emitted radiation or the Earth's reflected solar radiation is captured and converted to a digital image (Verhoeven, 2017). The interaction between electromagnetic energy and an object is also used in archaeological prospection. Remote sensing techniques are applied to discover archaeological remains, by means of

their response to electromagnetic energy. The following sections will elaborate on the theories behind thermography and multi-spectral imagery and their potential in the field of archaeology.

### 3.2 Aerial imagery

Aerial imagery is usually specified as a passive remote sensing technique. The data is acquired with an aircraft such as a drone or airplane. The thermal and multi-spectral data used in this thesis are both collected with a drone. Imaging derives from the interaction between electromagnetic radiation and the recorded object. Aerial imagery operates mainly in the optical electromagnetic spectrum, which can be divided into UltraViolet (UV), Visible (Vis) and InfraRed (IR). The reflectance of solar radiation can measure the visible part and shorter wavelengths of IR of the electromagnetic spectrum. Wavelengths from 6000 nm to 1.000.000 nm are estimated with the object's self-emitted thermal radiation (Verhoeven, 2017). This thesis utilizes thermography and multi-spectral data. Table 1 displays the division of the electromagnetic spectrum by wavelength and the imaging principles relevant to this thesis.

Optical electromagnetic radiation					
Division	Subdivision	Wavelength min (nm)	Wavelength max (nm)	Imaging principle	
<b>Visible (Vis)</b>	Blue (B)	400	500		
	Green (G)	500	600		
	Red (R)	600	700		
<b>InfraRed (IR)</b>	Near-InfraRed (NIR)	700	1 100	Solar-reflective spectral region	
	Short Wavelength InfraRed (SWIR)	1 100	3 000		
	Mid Wavelength InfraRed (MWIR)	3 000	6 000	Transition zone	Thermal region
	Long Wavelength InfraRed (LWIR)	6 000	15 000	Self-emitted thermal radiation	
	Far/Extreme- InfraRed (FIR)	15 000	1 000 000	region	

*Table 1. The division of optical electromagnetic radiation based on wavelength and the imaging principle (after Verhoeven, 2017)*

### 3.2.1 Thermography

Thermography is based on the distribution of thermal infrared radiation. Every material with a temperature higher than absolute zero (0 K or -273.15 °C) emits thermal radiation with wavelengths between 0.1 and 100  $\mu\text{m}$ . According to Stefan-Boltzmann's Law, the temperature of an object correlates to the emitted infrared radiation, which causes variability in temperature to be displayed by the distribution of thermal radiation (see Pappalardo et al., 2018). Figure 3 shows a schematic representation of the working principle of thermography. This image shows the most probable effect of thermal radiation emitted by architectural remains, pits, and ditches. However, this is highly influenced by the material, soil matrix and external factors, which should be considered in interpreting thermal anomalies (Casana et al., 2017).

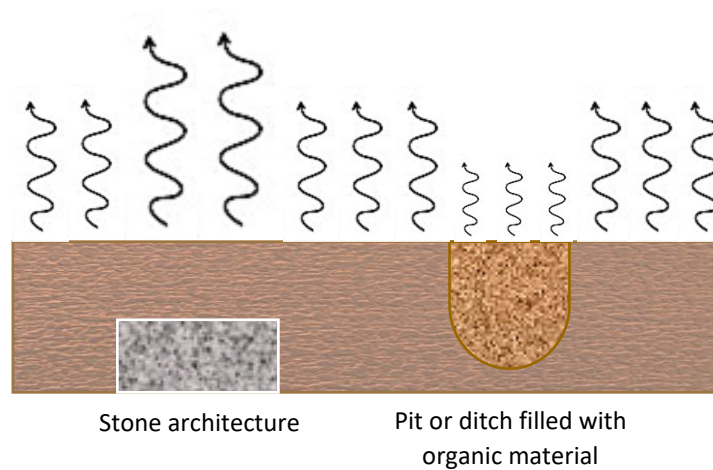


*Figure 3: Schematic representation of the working principle of thermography*

Anthropogenic features emit, absorb, reflect and transmit thermal radiation dissimilar to the surrounding soils. If the material's properties differ enough to show high contrasts on the thermal images, the archaeological features appear as anomalies on the thermograms (Casana et al., 2017; Cool, 2018; Pappalardo et al., 2018). The five variables that are most significant in defining the distribution of an object's thermal radiation are:

1. Thermal conductivity (W/mK): thermal conductivity measures a material's ability to transport thermal infrared energy. If the feature is buried underneath soil layers, it is necessary to have sufficient heat reach the anthropological feature. In this case, the soil matrix should have adequate thermal conductivity and be able to transport the thermal infrared energy to this depth, which makes it more likely that the feature shows up on the thermogram.
2. Thermal emissivity (0-1 scale): thermal emissivity marks the degree to which a material reflects or emits thermal radiation. If the emissivity of an archaeological object varies significantly from the surrounding soils, it might appear on the thermal images. Metals that

are unpainted or unoxidized are often used as ground control points. The low emissivity causes the points to appear as black spots on the thermogram.

3. Thermal inertia: thermal inertia describes the temperature flux of materials over 24 hours. Hence, thermal inertia is predominant in defining the optimal moment to collect thermal data and can be used to predict which materials will possibly show up on the thermogram.
4. Volumetric heat capacity: volumetric heat capacity specifies how much thermal radiation a unit volume of material needs to consume to increase its temperature by one-degree Celsius (Casana, et al. 2017; Cool 2018).
5. Thermal diffusivity: thermal diffusivity measures the rate at which temperature change transpires. The quicker heat transfers through a material, the lesser heat is absorbed. If the soil matrix has a high thermal diffusivity, more heat reaches the archaeological feature. In this instance, the temperature flux of the object is more dependent on its thermal properties and less limited by the properties of the soil (Cool, 2018).

These variables can be used to define which circumstances and materials are optimal for collecting thermal data for archaeological prospection. The interaction between the thermal radiation of an archaeological feature and its surrounding soil matrix was investigated by Périsset and Tabbagh (1981) by means of experimentation. Artificial features were analyzed by a software program to study how soil layers influence an object's thermal signature. The results are summarized by Cool (2018):

- An increase in thermal conductivity and a decrease in thermal diffusivity or an increase in thickness of the soil layer on top of the feature might cause the anomaly to become less apparent.
- The relative temperature of the feature is only affected by the properties of the anomaly and the soil matrix, not the surface layer.
- An increase in thermal conductivity or thermal diffusivity might cause the anomaly to be less visible.
- The strongest anomalies appear in subsoils with low thermal conductivity and low thermal diffusivity.
- The greater the contrast between the thermal inertia of the feature and its surrounding soil matrix, the stronger the thermal anomaly will appear on the thermogram

Besides the properties of the feature and soil matrix, thermal data is also affected by external factors such as environmental conditions, diurnal heat flux and drone height.

The importance of environmental conditions is described by Casana and colleagues (2017). Their case study in Kalavassos, Cyprus, highlighted the requirement of precipitation. Cyprus has a similar

Mediterranean climate as Greece, with wet winters and dry summers. During the data acquisition in Cyprus, the arid conditions caused the soil matrix to dry out and gain the same thermal properties as the buried stone architecture. The agricultural traces and aboveground topographic features were evident, but shallow archaeological features remained invisible.

Some of these factors were also investigated by Baroň, Bečkovský and Míča (2013), who applied infrared thermography to study the instability of rock slopes. They mention the negative impact of direct solar radiation on infrared thermography and establish that the ideal moment to capture thermal images occurs right before sunrise. The impact of direct insolation has been reaffirmed by Walker (2020), who defined the ideal conditions as shortly after sunset. In the case of heavy cloud cover, which limits sunlight refraction, the quality of the thermal images was even more enhanced. Another hypothesis involves the drone height. Baroň and colleagues (2013) noticed that the thermal contrast was significantly enhanced with a smaller height from the drone sensor to the ground surface, which was related to air humidity and the oblique position of the sensor.

### 3.2.2 Multi-Spectral Imagery

Multi-spectral imagery captures light at multiple wavelength ranges on the electromagnetic spectrum. These wavelengths are sampled in bands with different spacings and widths, which sometimes overlap. Multi-spectral imaging can capture wavelengths in both the visible and non-visible regions, thus also including Infrared and X-rays (Saleh, 2011). According to Saleh, the spectral bands used in research are strategically selected for domain-specific questions. The following generalizations are made:

- Blue light is generally used for underwater (to 45 meters) and atmospheric imaging applications
- Green light can be utilized in underwater (to 27 meters) and vegetation imaging applications
- Red light is often used for man-made objects, vegetation and soil applications
- Near-Infrared is applied to vegetation applications
- Mid-Infrared is generally used in soil, forest fires, vegetation, geological features and vegetation applications
- Far-Infrared Thermal Radiation is often utilized for imaging fires, oceanic temperature distributions and in night studies

Multi-spectral imaging is applied in a wide range of disciplines and the wavelengths used are highly dependent on the research aim as well as the availability of data.

Within archaeology, multi-spectral imaging is often applied to detect crop or soil marks. Cropmarks are caused by variations in the growth patterns of vegetation, which are indicated by crop color, leaf

area and stem height (Agapiou et al., 2013; Agudo et al., 2018; Themistocleous et al., 2015). Soil marks, on the other hand, can appear in bare soil regions. Differences in soil color or reflectance might indicate disturbances in the subsurface (Aqduş et al., 2012).

This thesis focuses only on cropmark detection. Cropmarks appear when the soil is disturbed, leading to differences in soil moisture, nutrients or rooting zone. Buried archaeological remains affect the growth pattern of crops by enhancing or limiting vegetation development. The cropmark also provides insight into the type of archaeological feature. In the case of a positive cropmark, this indicates a damp and fertile soil possibly caused by a trench, ditch or moat. At the same time, a negative cropmark suggests poor soils with few nitrates, induced, for example, by stone walls or foundations. However, cultivation practices, geological features, or geomorphological processes might also influence the development of crops. The interpretation of cropmarks depends highly on knowledge of the formation processes and possible archaeological features in the region (see Agapiou et al., 2013; Agudo et al., 2018; Themistocleous et al., 2015 and figure 4).

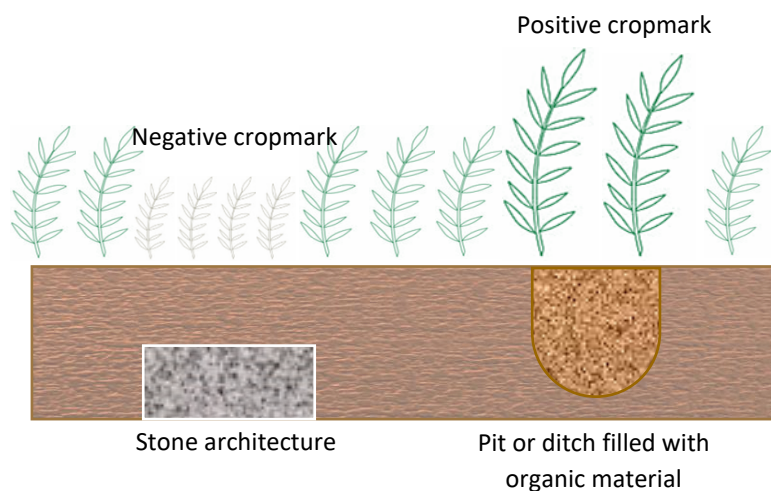


*Figure 4. A potential schematic representation of cropmarks caused by anthropological features*

According to Aqduş, Hanson and Drummond (2012), the detection of cropmarks depends on several external factors. They claim that an important variable is precipitation. In the case of constant rainfall, crops do not suffer from moisture deficiency and cropmarks are less apparent. Hence, the ideal conditions to discover cropmarks often occur in arid summers. However, this is very dependent of soil conditions, crop type and microclimates. Another factor is the type of vegetation. Deep-rooted agricultural crops produce the best results, but this is also influenced by other plant characteristics. Crop species have varying phenological cycles and they behave differently when exposed to increased or reduced moisture content. The last variable involves the soil type. For instance, the best results are achieved in well-draining soils, gravel and sand. Clay soils can provide good results if

rainfall is limited and the soil is not too saturated (Aqduş et al., 2018). Over all, it is difficult to define the ideal conditions to collect multi-spectral data, which is very variable and context dependent.

Crops have differing reflectance characteristics, which can be observed on the spectral bands of the electromagnetic spectrum. The aforementioned factors influence the reflectance characteristics. The near-infrared spectrum is an essential band in detecting the vegetation reflectance, but multi-spectral imagery is also used to collect data in the visible wavelengths (Agudo et al., 2018; Materazzi & Pacifici, 2022; Rondeaux et al., 1996).

Multi-spectral data is often used to create vegetation indices (VI), which combine the spectral bands employing mathematical formulas to provide information on the condition of crops. The VIs have been developed in the agronomy field to analyze specific traits of the studied crops. However, they can also improve the visualization of archaeological crop marks (Materazzi & Pacifici, 2022).

Vegetation indices (VI) combine the infrared and visible data to provide more specific information on vegetation growth. The most commonly used VIs are simple ratio (SR) and the normalized difference vegetation index (NDVI). However, these VIs are prone to external influences and new indices have been introduced to limit the influence of atmospheric effects, sunlight and soil properties (Huete, 1988; Materazzi & Pacifici, 2022; Nathalie Pettorelli, 2013; Pinty & Verstraete, 1992; Rondeaux et al., 1996). For more information on the vegetation indices used in this thesis, refer to chapter 4.

### 3.3 Geophysical prospection

Geophysical prospection has a long history within the field of archaeological survey. Geophysics originated as a subfield of archaeometry, which appeared from the 1950s to the 1960s. The 1970s saw a decline in geophysical techniques within the archaeological field, but significant technological advances by the late 1980s re-introduced the numerous possibilities of non-invasive techniques (Gaffney, 2008; Sarris, 2017). Geophysical prospection explores and measures the properties of the soil. These measurements are often taken at the surface to detect changes in the Earth's properties and processes. Changes in geophysical properties might indicate buried archaeological remains, which is why geophysics is gaining an increasing amount of attention as an archaeological prospection method (Sarris, 2017). This thesis employs the following geophysical techniques: Ground Penetrating Radar, Geomagnetic Survey, Electromagnetic Induction Survey and Earth Resistance Survey. The following paragraphs will discuss the theory and archaeological potential of these prospection methods.

#### 3.3.1 Ground Penetrating Radar

Ground Penetrating Radar (GPR) involves an electromagnetic geophysical technique that measures material properties using radio wave signals with frequencies ranging from 10 MHz to 2GHz. The GPR

instrument consists of an antenna, portable computer and timing unit. The antenna uses a transmitter and receiver to emit and detect electromagnetic signals. The timing unit measures the time between emitting and receiving the radar signals, which are stored and displayed on the portable computer. The transmitter emits high-frequency pulses into the subsurface. If the pulse encounters a different material, a part of the electromagnetic energy is reflected and recorded by the receiver. This process continues until all the energy is either reflected or absorbed by the soil (Annan, 2009; Gaffney, 2008; Manataki et al., 2015). Figure 5 illustrates the operation principle of GPR by displaying the paths of emitted radar signals.

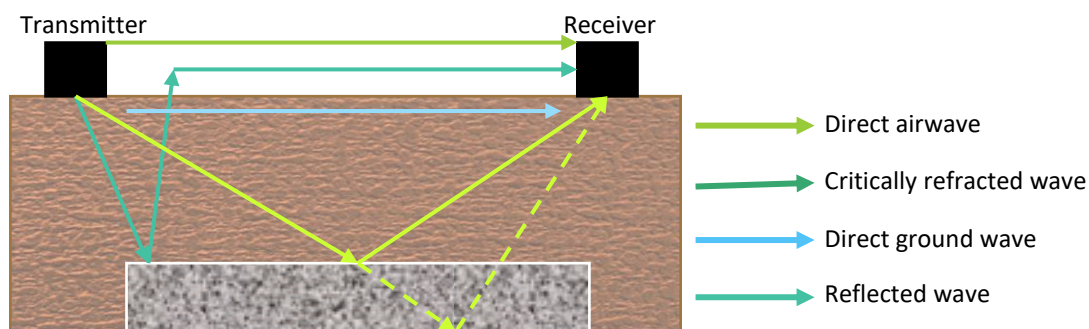


Figure 5. The working principle of Ground Penetrating Radar

GPR surveys are affected by soil properties. Knowledge of local soils is essential to assess the potential of GPR in a specific area. The reflectance of electromagnetic energy depends on differences between the electrical properties of the soils and buried materials. Conductivity and permittivity are the most significant properties. Conductivity defines the amount of energy absorbed and thus the maximum depth of the prospection, whereas permittivity influences the pace of the signals (Annan, 2009; Manataki et al., 2015). If the soil has high electrical conductivity, GPR penetration depths are decreased as the signals attenuate much faster in highly conductive soils. High conductivity values are often caused by clay particles, soil water or soluble salts. Hence if the soil is clay-rich, wet or saline, its GPR potential is significantly declined (Doolittle & Butnor, 2009; Manataki et al., 2015).

### 3.3.2 Geomagnetic Survey

Geomagnetic surveys capture fluctuations in the Earth's magnetic field. Buried archaeological remains interfere with the Earth's magnetic field, which produces weak local differences in the field strength or creates a new local field. There are two mechanisms that cause local variation in the Earth's magnetic field. The first process involves remnant magnetization, which can occur when a material is exposed to very high temperatures leading to permanent magnetization. The permanent magnetization causes a new local field, which can be measured with geomagnetic surveys. The other mechanism depends on a material's magnetic susceptibility. Magnetic susceptibility depends on the



content of iron oxides. An increased number of iron oxides appears on the magnetic data as a positive anomaly, whereas a decreased amount of iron oxides is depicted as a negative anomaly. A positive magnetic anomaly indicates that the feature has a higher magnetic susceptibility than the surrounding soil matrix, whereas a negative anomaly indicates the opposite. Geomagnetic surveys make use of a magnetometer or a gradiometer. Magnetometers measure the total field directly, which shows differences in the local field strength right away. Within archaeology, generally, a gradiometer is used. Gradiometers measure the magnetic gradient over a set distance. The gradient is affected by variation in the magnetic field caused by anomalies. Gradiometers are less impacted by the geology of the bedrock and the diurnal variations in the Earth's magnetic field (see Armstrong & Kalayci, 2015; Gaffney, 2008; Sarris, 2017 and figure 6).

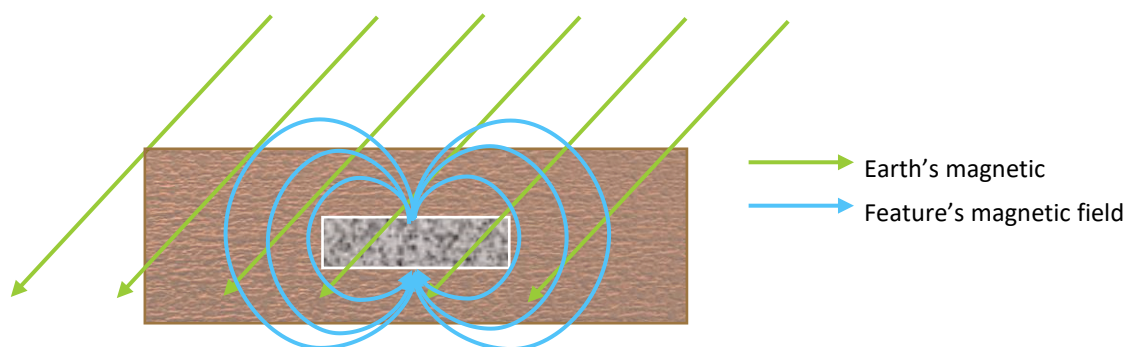


*Figure 6. A schematic representation of geomagnetic survey*

In the archaeological field, both remnant magnetization and enhanced magnetic susceptibility might cause anthropogenic features to appear on the geomagnetic data. Remnant magnetization often involves furnaces, kilns or fired bricks, and building materials created from magnetized igneous rocks. If a non-magnetic stone is used and its contrast with the more magnetic soil matrix is high enough, it might appear as a negative anomaly. Enhanced magnetic susceptibility appears in the materials that accumulate in pits, building fills, post-holes and ditches, which are represented as positive anomalies. The site type and materials can highly influence the quality of the geomagnetic data. If the contrast in magnetic values is too low, the visualization of archaeological remains will be problematic. Transient occupation sites, non-magnetic rocks with low contrast to the surrounding soil matrix and dry-stone walls often produce few results (Armstrong & Kalayci, 2015).

Besides the nature of the archaeological remains, the geology and environment of the research area are also of crucial importance when implementing a geomagnetic survey. The main problems are caused by waterlogged soils or igneous geology, whereas the areas most suitable for magnetic prospection contain sedimentary or metamorphic geologies (see Armstrong & Kalayci, 2015 and table 2).

Suitable / favourable	Unsuitable/problematic
Sedimentary parents including limestone, most sandstone	Igneous geology
Metamorphic geologies including slate, despite elevated background readings	Waterlogged soils
A few surveys have succeeded on basic igneous parents	Alluvium can be problematic, but depends heavily on local conditions: same for coversands, and clays
	Marine deposits such as old lagoons (good results from relict marine terraces however)

Table 2. Overview of suitable and unsuitable conditions for geomagnetic survey (Armstrong & Kalayci, 2015)

The Mediterranean climate provides good conditions for geomagnetic survey. The warm and dry summers produce oxidizing conditions, whereas the humid winters cause reducing conditions. The soils in this area have a high conversion rate of iron oxides, which generates strong contrasts in magnetic susceptibility (Armstrong & Kalayci, 2015).

### 3.3.3 Electromagnetic Induction Survey

Electromagnetic induction survey (EMI) measures the soil's conductivity, magnetic susceptibility and magnetic viscosity. The EMI device consists of a transmitter and a receiver. The transmitter coil creates an electromagnetic field with a frequency ranging from 8 to 90 kHz, but generally below 30 kHz. Buried materials interact with this field, producing a new electromagnetic field. The receiver coil detects this new field, which is divided into a quadrature and in-phase component. The quadrature component measures the material's conductivity, which is affected by the sensed material's porosity, water saturation, composition, and fluid chemistry. The in-phase component measures the magnetic susceptibility of the material, which is dependent on the concentration of magnetic materials. Magnetic viscosity corresponds to the quadrature component of susceptibility. The survey depth is defined by the distance between the transmitter and receiver coils as well as their orientation (see Sarris, 2017; Sarris et al., 2017; Simon, Tabbagh, et al., 2015 and figure 7).

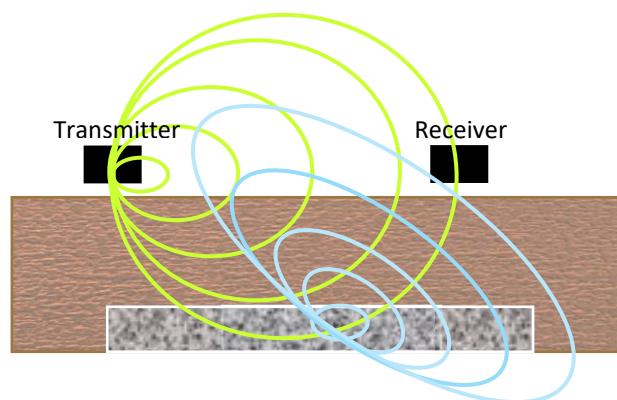


Figure 7. A representation of the electromagnetic induction principle

In this research, the GEM-2 instrument is used, which involves a multi-frequency device with two receiver coils in opposite directions. Simon and colleagues (2015) argue for the reliability of the GEM-2 in mapping conductivity, magnetic susceptibility and magnetic viscosity simultaneously.

Electromagnetic induction survey is widely applied in the detection of subsurface archaeological remains. Conductivity can be used to detect changes in soils and rocks, whereas magnetic susceptibility might indicate the development and erosion of the soil or reveal anthropogenic burning remains. Simon et al. (2015) applied multi-frequency EMI to two archaeological cases, which showed the significance of viscosity maps. They claim that magnetic viscosity is less valuable than susceptibility in the detection of archaeological features. However, if particular anomalies show up on the susceptibility maps but not on the viscosity maps, this could provide information on the composition of the construction material. The ratio between magnetic susceptibility and magnetic viscosity can be used to define the archaeological function of discovered features.

The potential of electromagnetic induction surveys in discovering and interpreting archaeological features is widely known. According to Sarris (2017), EMI can easily expose high moisture areas, artificial pits and metal objects. This is substantiated by a large number of case studies (Rodrigues et al., 2009; Simon, Tabbagh, et al., 2015; Tang et al., 2018). However, Zheng and colleagues (2013) also mention that electromagnetic systems are best used in general surveys to select areas for a more detailed investigation. Another advantage of electromagnetic induction is that it can be collected without direct contact with the topsoil, which is convenient in surveying large areas (Sarris et al., 2017).

#### 3.3.4 Earth Resistance Survey

According to El-Qady and colleagues (2018), earth resistance survey was the first prospection technique applied within the field of archaeology. Since then, it has been widely used to detect archaeological remains.

Resistance survey is based on the electrical properties of materials. Electrodes are used to inject an electrical current into the ground, which is measured when it returns to the surface. The electrical current is altered by buried objects and different soils, depending on their electrical properties. The main property includes electrical resistivity, which measures the obstruction of movement of ions within a material. The transport of ions is affected by salt and moisture content. Salts release ions when dissolved, after which they are transferred through the soil by water. Resistance survey is thus mainly affected by soil moisture. However, temperature also influences the transport of ions. Lower temperatures cause a decrease in ion mobility and frost ceases ion movement (see El-Qady et al., 2018; Moffat, 2015; Schmidt, 2013 and figure 8).

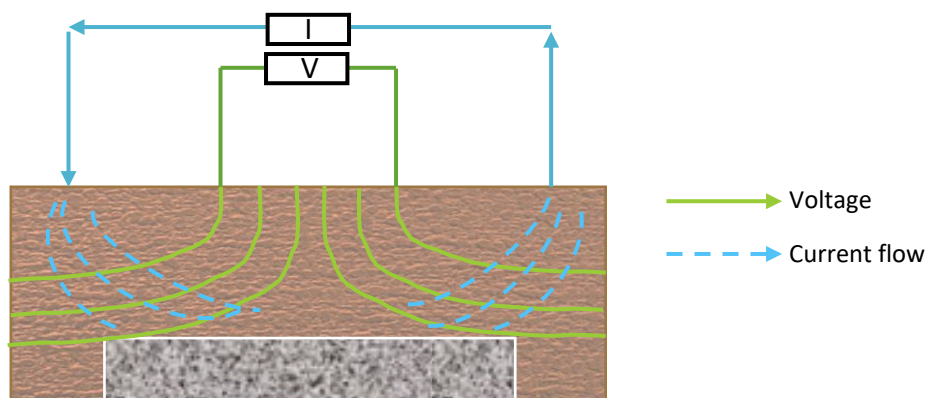


Figure 8. A schematic representation of earth resistance survey

Within archaeological prospection, earth resistance survey can be applied to discover buried archaeological remains. Archaeological features alter the electrical current, which can be measured with the prospection device. However, the detectability of archaeological remains depends on the resistivity contrast between the feature and its soil matrix. As indicated before, resistivity is primarily determined by a material's moisture content. High contrast in resistivity thus corresponds with high contrast in water content, which can cause either a positive or a negative resistivity contrast. Stone foundations could show a positive resistivity contrast. They generally contain low levels of moisture, which is reflected by high resistivity values. The surrounding soil matrix holds significantly more moisture, causing low resistivity values. On the other hand, ditches are often revealed as negative resistivity contrasts. After use, the ditch is filled with different soils, either by human or nature. These soils are less densely packed and have larger pores, making it easier to contain water. This results in resistivity values lower than the surrounding soil matrix (Schmidt, 2013).

However, the interpretation of earth resistance anomalies must be carefully considered since soil moisture is highly affected by environmental factors and weather circumstances. Smith (2013) discusses the effect of external factors on the detectability of archaeological remains. The following observations were made.

- If the summer is hot and dry, the contrast might be enhanced. The soil matrix dries out, whereas the ditch remains moisturized. However, if the heat continues for a long period, the ditch content also dries out. Consequently, the contrast might disappear, making it impossible to detect the ditch on the earth resistance data.
- The same situation occurs with heavy rainfall. Heavy rain might enhance the negative contrast of a ditch. However, if the rainfall continues for an extended period, the complete soil would be soaked and the contrast disappears.

- In the case of sun and force winds, evapotranspiration occurs in the ditch and soil matrix. The large pores of the ditch content cause stronger evapotranspiration than the surrounding soil, which leads to a positive contrast.

These observations show that earth resistance survey depends on environmental circumstances and that knowledge of the weather conditions is crucial for interpreting positive and negative contrasts. However, it needs to be kept in mind that anomalies do not necessarily indicate archaeological remains and might be explained by geological features (Schmidt, 2013).

### 3.4 Concluding remarks

This chapter provided a consolidated overview of the theory behind the six remote sensing techniques that are applied on Voulokaliva and aimed at answering the question: What are the ideal conditions to collect data with six respective remote sensing technologies and how can this knowledge be applied in archaeological prospection?

An extensive literature review discusses the theory behind thermography, multi-spectral imagery, ground-penetrating radar, geomagnetic survey, electromagnetic induction survey, and earth resistance survey. The ideal circumstances to collect each respective dataset are addressed, including vegetation, soil matrix and environmental conditions. This information is specified for archaeological prospection by assessing the impact of external factors on archaeological features. This theoretical framework will be applied to the results of the remote sensing data from Voulokaliva in chapter 5.

## 4. Methodology and approach

The following chapter will provide the methodology as applied in this research. This study aims at comparing a variety of remote sensing techniques and assessing which techniques prove most valuable at Voulokaliva in Halos, Greece. The first section discussed the materials used in this research and their contribution to the project. The materials consist of fieldwalking surveys and remote sensing data. The datasets are combined into a QGIS file, which is used to visualize, analyze and compare remote sensing data. Second, the individual layers are analyzed and potential anomalies are highlighted on each unique dataset. The last stage of research consists of a comparative approach, in which the anomalies observed with each technique are compared. The methodology applied is expected to demonstrate the possibilities and limitations of remote sensing techniques within archaeological prospection and shed light on the preferable methods in the Voulokaliva area.

### 4.1 Materials

The survey data is accumulated by means of a literature study, mainly focused on the book by Reinders (2004): *Prehistoric Sites at the Almirós and Soúrpi Plains (Thessaly, Greece)*. This book provides a concise summary of the discovered archaeological remains at Voulokaliva. Voulokaliva has been the subject of multiple archaeological prospection campaigns. The earliest data consists of fieldwalking surveys dating from 1990 to 2006. During these campaigns, the area was covered by a team of archaeologists and students by systemic fieldwalking. A large number of finds were collected, counted and documented, which indicates the archaeological potential of the area (H. Reinders, 2004). As mentioned in chapter 2, the site was revisited by Stissi and colleagues (2015) in 2011-2013. All accessible areas were subject to a more refined and intensive fieldwalking survey (figure 1). The survey results guide the interpretation of remote sensing data and provide the site with a chronological framework.

The majority of the dataset consists of remote sensing data, specifically thermography, multi-spectral imagery, ground-penetrating radar, geomagnetic survey, electromagnetic induction survey and resistivity. The thermal and multi-spectral data are collected by an Remotely Piloted Aircraft System (RPAS) and are therefore classified as aerial imagery. The thermal data is used to locate temperature differences in the subsoil, which might indicate the presence of archaeological disturbances. Multi-spectral imagery is applied to enhance the visualization of cropmarks caused by anthropological features. Both aerial imagery methods can thus be used to detect archaeological remains with a relatively high resolution. The thermal and multi-spectral data is collected by Jitte Waagen and colleagues from the 4D Research Lab in Amsterdam. The aerial images were captured from different

heights and seasons to compare remote sensing data captured under different circumstances. Appendix I contains the details and environmental circumstances of the different drone flights and corresponding thermal or multi-spectral datasets. Optical data is also collected, which will be used to check if potential archaeological anomalies are produced by objects above ground.

The other datasets are categorized as geophysical prospection. Ground-penetrating radar uses electromagnetic frequencies to locate objects in the subsoil by emitting and detecting waves reflected by the different materials. This technique can be used to detect archaeological features and estimate their depth. Geomagnetic survey measures the strength of the magnetic field of the Earth. Buried archaeological remains cause changes in the local electromagnetic field or create a new local field that influences the Earth's magnetic field (Armstrong & Kalayci, 2015; Sarris, 2017). The electromagnetic induction survey consisted of electrical conductivity, viscosity and magnetic susceptibility. These methods can aid in locating interesting archaeological areas and provide information on palaeolandscapes (Armstrong & Kalayci, 2015; Sarris, 2017). In this research, the electromagnetic survey is used to compare potential archaeological areas with the location of anomalies detected with other remote sensing techniques. The last technique is resistance survey, which measures the resistance of the soil. Low- or high-resistance anomalies might indicate the presence of archaeological features such as voids, organic materials or stone objects (Sarris, 2017). The geophysical data was collected by Apostolos Sarris and his team in the Spring of 2015 (Sarris et al., 2016). The details of the geophysical survey are indicated in appendix II and the orthophoto is used to check the geophysical anomalies with potential obstructions above ground.

## 4.2 Methodology

The thermal images are first entered into Pix4D software which uses photogrammetry and algorithms to transform the images into thermal 2D and 3D models. The 2D models are compiled in a QGIS file and the individual datasets are analyzed to improve the visibility of potential anomalies. Several QGIS tools are applied to enhance the thermal and multi-spectral data. The thermal data is visualized with different color ramps, such as Viridis, Magma and RdGy. The Local Cumulative Cut Stretch in the raster toolbar of QGIS is used to vary the minimum and maximum values of the raster histogram (Kokalj & Hesse, 2017; Kokalj & Somrak, 2019). The multi-spectral datasets are added to the same QGIS file. This thesis utilizes four vegetation indices, to enhance the detectability of cropmarks. Materazzi and Pacifici (2018) demonstrate that the VIs that produced the best results are the indices that use the red and near-infrared spectrums. According to Agudo et al. (2018), the green band might also provide interesting results since this spectral range is related to chlorophyll content, which could be affected by buried archaeological remains. Hence, this thesis uses four indices calculated with the red, near-infrared and green bands. The data was collected in August and

November 2021, of which the timing was determined by fieldwork seasons. Future drone flights will be performed at different periods. Nevertheless, this research is restricted to the data collected in August and November. The Sentinel-2 data discussed in chapter 2 indicated a low amount of vegetation in August and varying vegetation coverage in November at Voulokaliva site 1990/35. The application of vegetation indices in areas without vegetation might not produce any results. Nevertheless, the detection of archaeological anomalies in areas with low to moderate vegetation coverage could be enhanced by employing vegetation indices, which also facilitates an assessment of vegetation indices in areas with limited vegetation. Table 3 presents the VIs, formulas and related possibilities and limitations used in this research. The VIs are calculated with the Raster Calculator tool in QGIS.

<b>Vegetation Index Abbreviation</b>	<b>Vegetation Index</b>	<b>Formula</b>	<b>Possibilities</b>	<b>Limitations</b>	<b>References</b>
NDVI	Normalized Difference Vegetation Index	$(\text{NIR} - \text{Red}) / (\text{NIR} + \text{Red})$	Increase contrast between soil and vegetation, less sensor calibration degradation, extensively used in archaeological prospection	Sensitive to the atmosphere, soil brightness, soil variations and illumination are also less useful in dense vegetation	(Huete, 1988; Nathalie Pettorelli, 2013; Pinty & Verstraete, 1992; Rondeaux et al., 1996)
GNDVI	Green Normalized Difference Vegetation Index	$(\text{NIR} - \text{Green}) / (\text{NIR} + \text{Green})$	Sensitive to chlorophyll content	Mainly effective in green vegetation which photosynthesizes	(Agudo et al., 2018; Materazzi & Pacifici, 2022)
SAVI	Soil Adjusted Vegetation Index	$(\text{NIR} - \text{Red}) / (\text{NIR} + \text{Red} + 0.5) \times (1 + 0.5)$	Reduced noise from soil variation (soil brightness and orientation)	Soil noise with high chromas is not minimized	(Agudo et al., 2018; Huete, 1988; Rondeaux et al., 1996)



GEMI	Global Environment Monitoring Index	$GEMI = \eta \times (1 - 0.25 \times \eta) - ((Red - 0.125)/(1 - Red))$ $\eta = (2 \times (NIR^2 - Red^2) + 1.5 \times NIR + 0.5 \times Red)/(NIR + Red + 0.5)$	Less influenced by atmospheric and illumination conditions, contains the same information on crop characteristics as NDVI	The formula is very complex and hard to interpret	(Pinty & Verstraete, 1992; Rondeaux et al., 1996)
------	-------------------------------------	---	---	---	---

*Table 3: An overview of the vegetation indices that are used in this research*

After the VI's are calculated, the thermal and multi-spectral data is visually explored for potential archaeological remains. Interesting areas or shapes are marked and two vector files are created for the discovered anomalies in the thermal and multi-spectral data. The geophysical datasets already consist of vector data, displaying potential archaeological anomalies as interpreted by Sarris. The processed data is visualized in the technological report and can be used to interpret and critically assess the drawn anomalies (Sarris et al., 2016). The vector datasets are used in a comparative approach, elaborated upon in the following paragraph.

### 4.3 A comparative approach to remote sensing techniques

A comparative approach is used to assess the potential of the different remote sensing techniques at Voulokaliva. The vector datasets containing the anomalies are overlaid and corresponding shapes are highlighted. The results are discussed in the context of the site and the theory behind the remote sensing techniques. If anomalies appear on multiple datasets, the buried material has properties that can be captured with different sensors. On the other hand, if anomalies only show up on one dataset, there are two hypotheses'. Either the anomaly is false and produced by problems during data capturing or processing, or the anomaly is only sensitive to a particular remote sensing technique. The comparative approach is thus also used to validate the observations. If an anomaly appears on multiple datasets, the possibility of it being a potential archaeological feature increases. However, it needs to be kept in mind that remote sensing is classified as a prospection technique and excavation is still necessary to confirm the presence of archaeological remains.

## 5. Results

This chapter will address the results of both the remote sensing data and the comparative approach. The aerial images are scanned for anomalies that might indicate archaeological remains. The geophysical data has already been analyzed by Sarris et al. (2016) and the results will be discussed, considering the processed data. The second section presents the results of the comparative approach, in which the anomalies detected on the aerial images and geophysical data are cross-checked. The similarities and differences between the datasets are addressed in the context of Voulokaliva. This chapter aims at answering the following sub-question proposed in the introduction:

- Which anomalies can be detected on the remote sensing imagery and how do they compare to each other?

### 5.1 Results of the remote sensing data

#### 5.1.1 Thermography

The thermal data consists of two datasets captured in August at 40 and 80 meters aboveground. The dataset collected at the height of 40 meters only covers the southwestern part of Voulokaliva, whereas the 80 meters dataset includes the entire site.

The thermal dataset collected at the height of 80 meters showed two large anomalies in the eastern part of the research area. The anomaly on the left (3) measures 18 by 7.5 meters and is oval-shaped, with another smaller anomaly (4) in the middle. The anomaly on the right (1) measures 24.5 by 19.5 meters and is square-shaped. The second anomaly contains a small square-shaped anomaly (2), measuring five by seven meters.

Due to the olive trees located in the northwestern part of the site, this area did not show any thermal anomalies. The southwestern area, however, displayed some potential archaeological features. A semi-circular anomaly (5) is apparent in the center of this region, measuring nineteen by eight point five meters. In the middle, another smaller circular anomaly (6) is visible. The other anomalies in the area are less evident. The southern part of the region indicates some warmer regions with angular and rectangular shapes (7) (see figure 9).

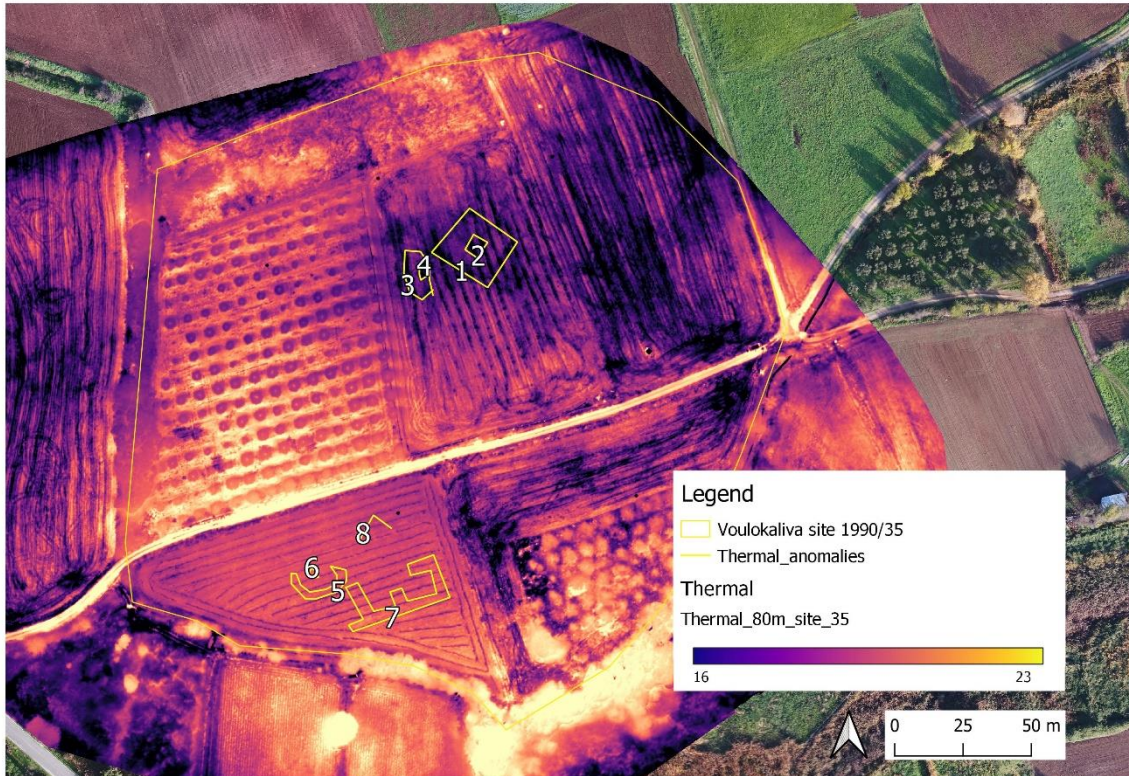


*Figure 9. The thermography results of Voulokaliva site 1990/35, positioned on the thermal and optical data collected in August*

### 5.1.2 Multi-Spectral Imagery

The multi-spectral data was collected in August and November at the height of 40 and 80 meters, covering the entire research area. The November dataset reveals positive circular anomalies (12-16) at the top of the northeastern part of the research area, their diameter ranging from 3.5 to 7.5 meters. A negative angular anomaly (17) is located below these pit-like anomalies. Another remarkable cropmark can be found at the edge of the olive tree field. The anomaly measures 25 meters in width and 22 meters in length and shows a negative cropmark (8). The November data also suggest a semi-circular positive anomaly (97) in the western part of the olive tree region. The southern regions did not display any anomalies in the November data (see figure 10 and figure 11).

The August data did not indicate any anomalies in the northern part of the site. In the southwestern part of the research area, some darker areas suggest the presence of negative cropmarks. The western side of the region seems to display a linear anomaly (11), which extends for 26 meters. However, the agricultural traces make it difficult to establish a clear pattern (see Stissi et al., 2015, figure 12, and figure 13).

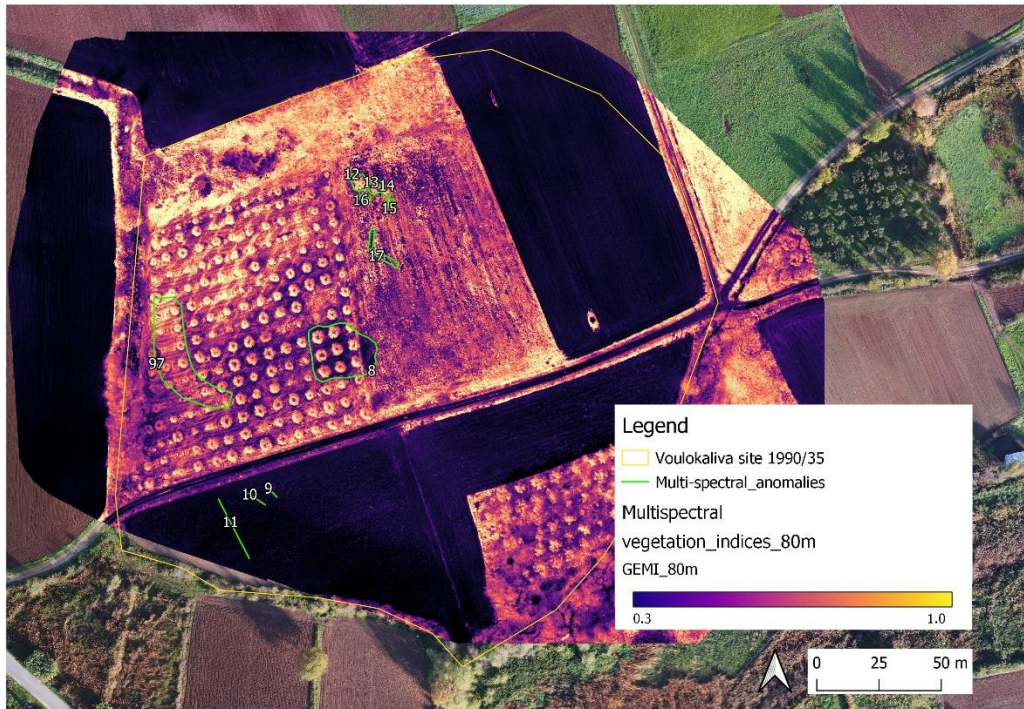


Figure 10. The multi-spectral imagery results of Voulokaliva site 1990/35, superimposed on the multi-spectral data collected in November (GEMI )



Figure 11. The multi-spectral imagery results of Voulokaliva site 1990/35, superimposed on the multi-spectral data collected in November (NDVI)

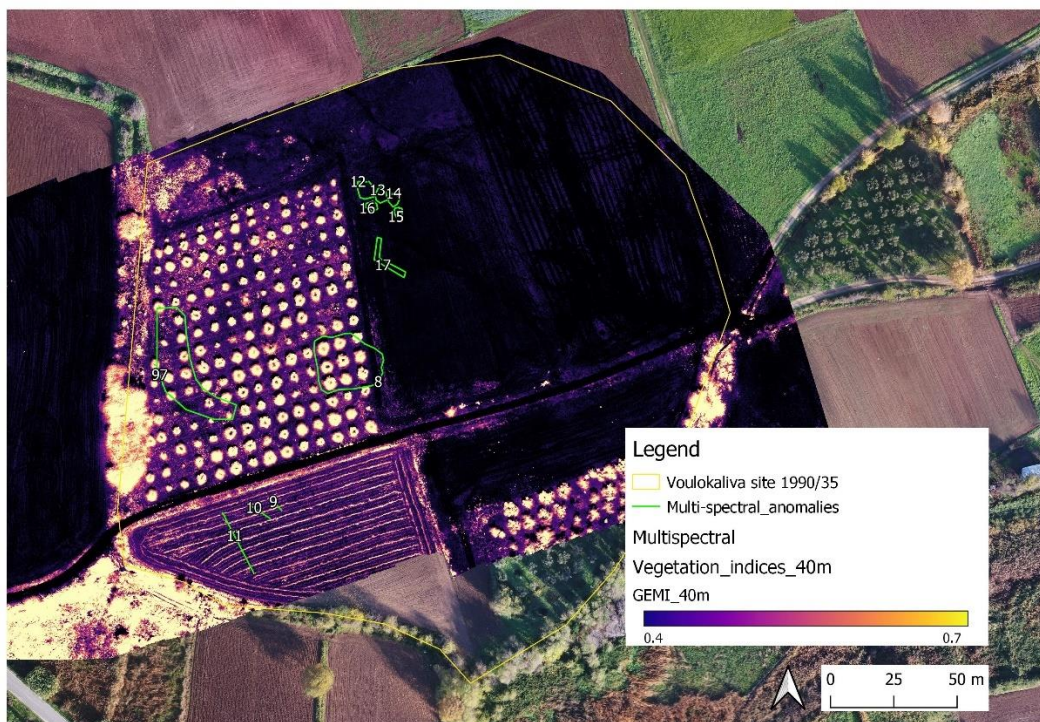


Figure 12. The multi-spectral imagery results of Voulokaliva site 1990/35, superimposed on the multi-spectral data collected in August (GEMI )

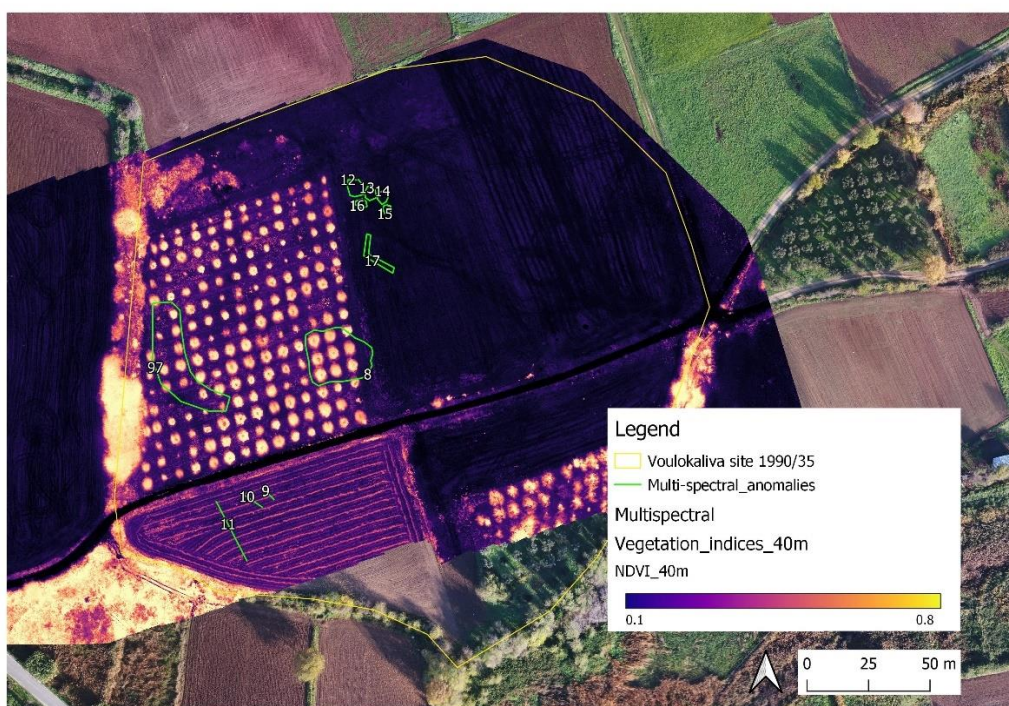
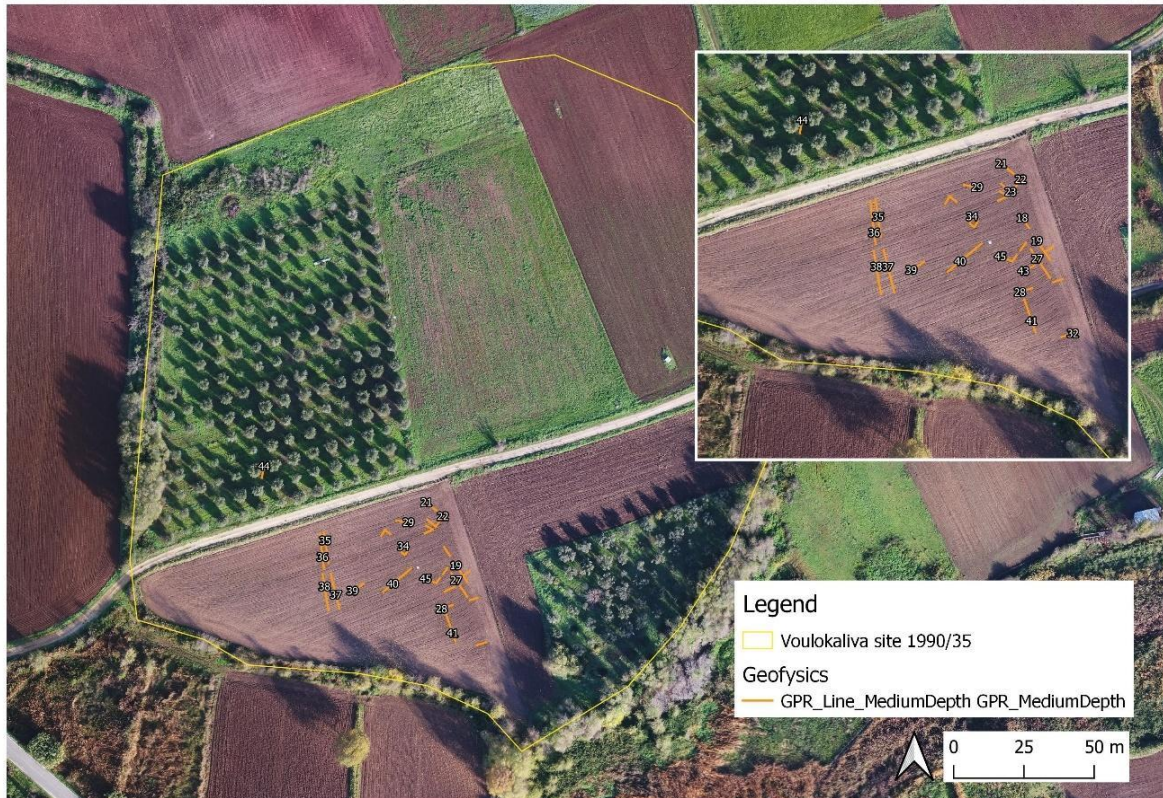


Figure 13. The multi-spectral imagery results of Voulokaliva site 1990/35, superimposed on the multi-spectral data collected in August (NDVI)

### 5.1.3 Ground Penetrating Radar

The ground-penetrating radar data was solely collected in the southwestern grid and a small part of the northwestern grid. In the northern grid, no anomalies were indicated, whereas the southern grid contained a large number of potential archaeological remains. The depth slice that produced the best results was located at 80 to 90 centimeters, on which Sarris and colleagues highlighted multiple anomalies (see Sarris et al., 2016 and figure 14).



*Figure 14. The ground-penetrating radar results of Voulokaliva site 1990/35, positioned on the optical data collected at the height of 250 meters (after Sarris et al., 2016)*

Numerous linear anomalies were detected, the most evident being 35, 36, 37 and 38. These anomalies form 2 parallel lines and extend for more than 25 meters in the north-southern direction. The south-eastern part of the surveyed field is densely packed with several linear anomalies located at a depth from 50 to 140 centimeters below ground. The linear and angular nature of the features suggest walls and roadways; in addition, the strength of the reflectors implies stone-based foundations (Sarris et al., 2016).

#### 5.1.4 Geomagnetic Survey

The geomagnetic survey data were collected at the western part of Voulokaliva. A large number of circular anomalies were detected, distributed across the entire survey area. The circular anomalies in the southwestern part of the site consist of dipole anomalies. Also, a high amplitude of circular anomalies in the northeastern and southeastern areas becomes apparent and the southeastern part contains some linear and angular anomalies. The circular anomalies are not included in the vector dataset, but they are discussed in the technical report by Sarris and colleagues (2016).

However, the most evident anomalies are located on the western side of the surveyed region. Two parallel semi-circular features are placed 13 to 16 meters apart and extend for about 170 meters. The outer anomaly (47) has a width of approximately four meters, whereas the inner anomaly (50) has a width of two meters. Another linear anomaly (52) is visible, crossing the aforementioned potential ditches (see Sarris et al., 2016 and figure 15).

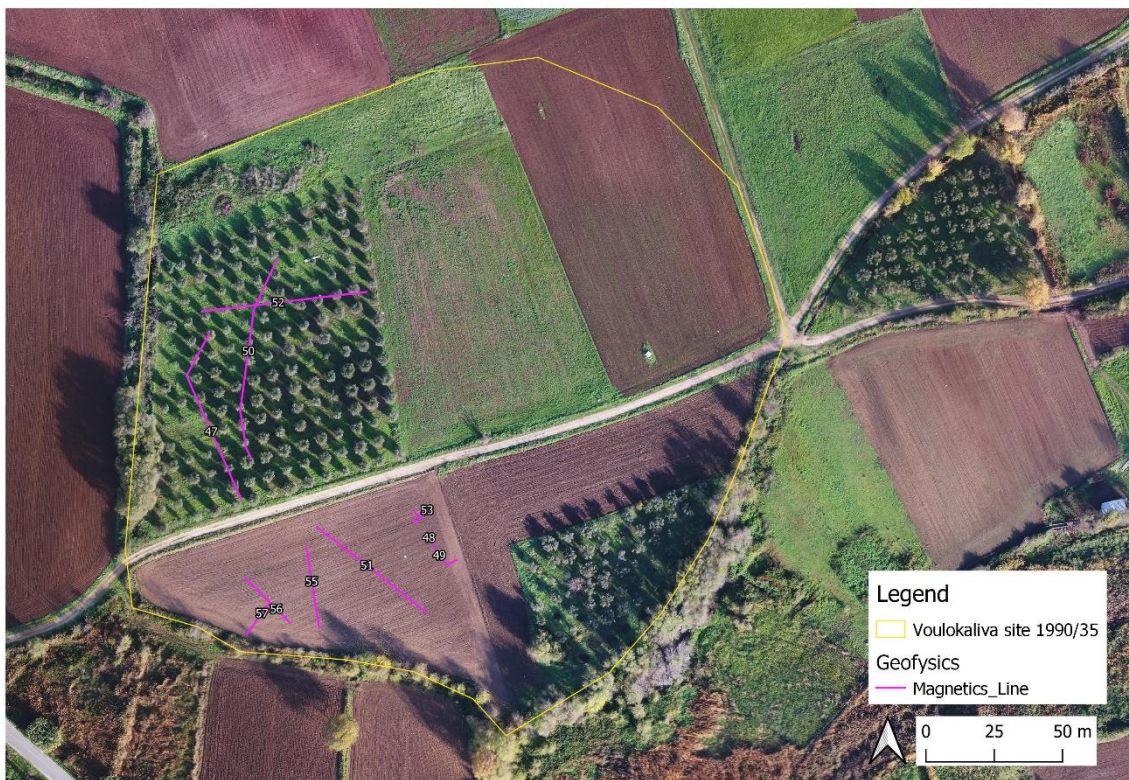


*Figure 15. The geomagnetic survey results of Voulokaliva site 1990/35, superimposed on the optical data collected at the height of 250 meters (after Sarris et al., 2016)*

#### 5.1.5 Electromagnetic Induction Survey

The electromagnetic induction survey at Voulokaliva included conductivity, viscosity and susceptibility measurements. The northwestern part of the site contained three areas with

particularly low conductivity, low susceptibility and high magnetic viscosity values. These regions might suggest anthropogenic activity, which appears to continue in the southern area below the modern road (see Sarris et al., 2016 and figure 16).



Figure 16. The electromagnetic induction survey results of Voulokaliva site 1990/35, positioned on the optical data collected at the height of 250 meters. From left to right: conductivity, viscosity and susceptibility at the frequency of 43350 Hz (TOP) and the interpretation of the anomalies (BOTTOM) (after Sarris et al., 2016)

### 5.1.6 Earth Resistance Survey

The earth resistance survey was conducted solely in the southwestern region of Voulokaliva. A number of anomalies with high resistance values appeared. The processed data shows rectangular-shaped anomalies and linear anomalies. The anomalies are distributed inconsistently, but the clustering of features does imply the presence of a settlement (see Sarris et al., 2016 and figure 17).





Figure 17. The earth resistance survey results of Voulokaliya site 1990/3, overlaid on the optical data collected at the height of 250 meters (after Sarris et al., 2016)

## 5.2 Results of the comparative approach

The remote sensing data of Voulokaliya is subjected to a comparative evaluation of the discovered anomalies and potential archaeological remains. This comparative approach is highly influenced by the availability and quality of the remote sensing data. If data from a specific region is missing or lacks the quality to obtain reliable results, the corresponding remote sensing technique will not be discussed in the assessment of that particular area. The geophysical prospection was restricted to the western part of the site. However, the aerial imagery was affected by the presence of the olive trees, and limited results were produced in the northwestern region. The north-eastern part of the research area did deliver several thermal and multi-spectral anomalies, but no geophysical prospection was applied here. The southwestern part of the site produced numerous aerial imagery and geophysical prospection results. The following section will discuss the results of the comparative analysis more in-depth. For an overview of all anomalies detected on the different remote sensing datasets, refer to figure 18.

The highest correlation of potential archaeological remains appears in the southwestern part of the research area. Ground-penetrating radar, geomagnetic survey and earth resistance survey

highlighted several linear and angular anomalies in this area (Sarris et al., 2016). The orientation and shape of the anomalies are significantly similar and indicate the presence of stone structures or foundations. On the thermal data, multiple warmer regions with angular and rectangular shapes appear in this area, which also can be linked to structural remains. In the western part of this region, multi-spectral and geomagnetic data indicate a linear anomaly, which corresponds with an area of high susceptibility.

Another interesting correspondence appears in the northwestern part of the site. The linear anomalies found in the geomagnetic dataset are located at the boundaries of the low conductivity and high viscosity polygons. The olive trees in this area disturbed the aerial imagery data, which made the discovery of anomalies more challenging. However, on the multi-spectral data collected in November, an area of high multi-spectral values becomes visible at the same location as the aforementioned geophysical anomalies. These anomalies can be linked with the linear anomalies in the southwestern part of the site.

The northeastern part of Voulokaliva was only investigated by drone and no ground-based geophysical technique was applied here. However, the circular anomalies distinguished on the multi-spectral data in the most northern part of the region correspond with Sarris’s circular anomalies slightly to the West on the geomagnetic dataset. A noticeable observation involves the significantly different results from the multi-spectral and thermal data. The large ditch-like features on the thermal data of August are not visible on the multi-spectral data from both August and November. Also, the circular ditches on the multi-spectral data of November do not show up on the thermal data of August. However, thermal anomaly three and multi-spectral anomaly 17 have similar shapes and are located in the same area.

Table 4 provides an overview of the anomalies (as numbered in figure 18) which appear on multiple datasets and their respective length in meters. If the anomaly is not a line, the polygon’s diameter is measured. Table 4 shows the highest correlation between ground-penetrating radar and geomagnetic survey.

Thermal	Multispectral	Ground Penetrating Radar	Geomagnetic Survey	Electromagnetic Induction Survey	Earth Resistance Survey
		18 [3.7]	48 [4.6]		
		19 [4.8] & 20 [2.9]	49 [4.6]		
		21 [5.9]			58 [4.4]
		22 [5.0] &	53 [6.9]		59 [13]

		25 [3.2]			
		23 [3.9]	54 [3]		
		36 [12.5] & 38 [12.7]	55 [29.4]		
	11 [26.7]		56 [23.3]	S2 [37.0]	
	97 [50.0]		47 [68.0]	CL3 [70.5] & V2 [75.0]	
			50 [75]	CL2 [36.0] & V2 [75.0]	
3 [18.5]	4 [17.5]				
5 [19.5]					87 [4.2] & 83 [4.7]
7 [38.2]		28 [4.2] & 43 [4.0]			67 [7.4] & 68 [7.3]
8 [18.2]		30 [2.5] & 31 [2.5]			

Table 4. An overview of the anomalies on multiple datasets and their respective length in meters, the numbers can be read as: anomaly\_number [length in meters]

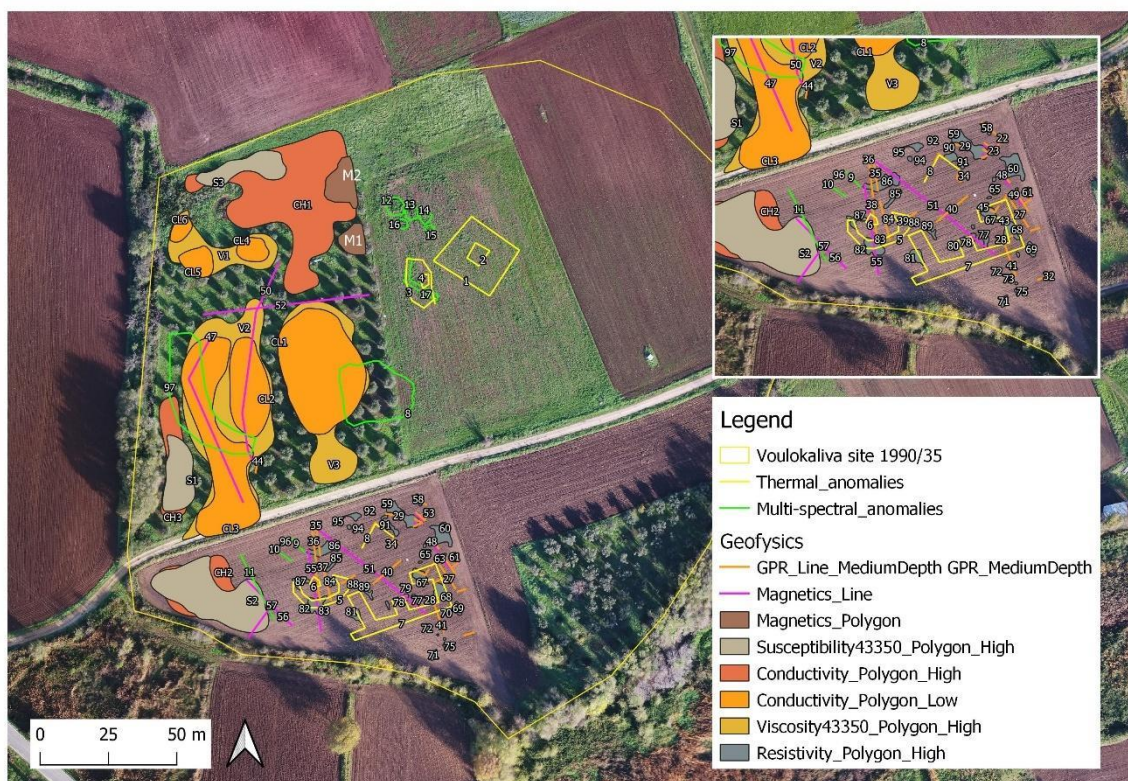


Figure 18. Comparison of all discovered anomalies superimposed on the optical dataset collected at the height of 250 meters

### 5.3 Concluding remarks

This chapter reviewed the results of the remote sensing techniques at Voulokaliva and the subsequent comparative analysis. The thermal and multi-spectral data did not uncover many anomalies. However, the geophysical prospection did reveal a large number of potential archaeological features. The southwestern region was covered by all geophysical surveys and consequently provided the most results. The comparative analysis showed a significant correlation between ground-penetrating radar and geomagnetic survey anomalies, yet the anomalies discovered with the other techniques also demonstrated similarities. The results of both the remote sensing techniques and the comparative approach will be elaborated upon and discussed in the following chapter.

## 6. Discussion

This chapter will discuss the results of chapter 5. The first section will reflect on the anomalies discovered by the remote sensing data. The results are addressed in relation to the theoretical background of the different techniques, as outlined in chapter 3. The subsequent paragraph will elaborate on the interpretation of the results and the importance of the researcher's bias, expertise and experience. The discussion will focus on both the individual remote sensing results and the outcome of the comparative analysis. This chapter aims at answering three sub-questions:

- How do the detected anomalies relate to the theoretical background of the applied remote sensing techniques?
- To what extent do the anomalies correspond to the hypotheses based on previously executed field survey campaigns?
- Which remote sensing techniques prove the most effective in visualizing archaeological cropmarks at Voulokaliva site 1990/35?

### 6.1 Reflecting on the results

A clear distinction can be made between the aerial imagery and the geophysical prospection results when looking at the individual remote sensing data. Both the thermal and multi-spectral datasets produced a limited number of anomalies and the interpretation proved difficult, whereas the geophysical prospection yielded a large number of potential archaeological features. This section elaborates on the relation between the detected anomalies and the theoretical background of the respective remote sensing technique.

#### 6.1.1 Aerial imagery

Theoretically speaking, the moment of data collection should produce good thermal results since the drone flight was carried out after dusk (Baroň et al., 2013; Walker, 2020). However, the thermal data did not expose many anomalies. One issue involved the olive trees in the northwestern part of the research area, which prevented the discovery of archaeological remains. The thermal data revealed some ambiguous ditch-like features in the north-eastern and southwestern regions, but the large number of agricultural traces significantly decreased the uncovering of anomalies. The tractor marks in the southwestern part of the research area, for instance, are difficult to distinguish from potential archaeological anomalies. The limited findings might also be explained by the soil matrix and the environmental conditions. As mentioned by Casana and colleagues (2017), both arid conditions as clay-rich soils proved unsuitable for the discovery of thermal archaeological anomalies. The dry

summer at Voulokaliva in combination with the presence of clay particles, might have hindered the uncovering of archaeological remains. In addition, chapter 2 identified periods of extreme drought in Thessaly from the mid-1970s onward (Loukas et al., 2008). Persistent aridity causes the soil matrix to dry out, which reduces the contrast between archaeological anomalies and the surrounding soil (Casana et al., 2017).

The anomalies detected on the multi-spectral data are significantly different on each dataset. The data collected in August only showed anomalies in the southwestern region, whereas the data acquired in November only exposed potential features in the northern region. Similar research by Aqduş and colleagues (2012) mentions that constant rainfall prevents moisture stress in crops, and therefore the ideal conditions to acquire multi-spectral data often occur in dry summers, with deep-rooted agricultural crops and well-draining soils. It needs to be kept in mind that these conditions are very context dependent and the Voulokaliva area might produce different results. The deposits in the Voulokaliva area contain a high degree of leaching and according to Aqduş et al. (2012) the clay soil could provide precise results if not too saturated. Palmer (2007) provides an example of clay soil under dry weather circumstances, which indeed generated cropmarks. Both the August and November data was collected in an arid period with some occasional rain. The clay soil was thus probably not too saturated, which should not cause problems for the multi-spectral data. However, the main component in multi-spectral imagery involves the phenological stage of the crops during data acquisition. Sentinel-2 data showed a lack of vegetation in August and the varying vegetation coverage in November. This was confirmed by the optical datasets collected by Jitte Waagen and colleagues. In August, the southwestern part of the site contains initial crops, whereas the northeastern and southeastern regions do not indicate any vegetation. In November, however, the northeastern area shows vegetation, and the cropmarks detected with the multi-spectral imagery are even visible on the optical dataset. The southeastern and southwestern regions, on the other hand, do not display any vegetation. Figure 19 shows the multi-spectral data collected in August and November, which clearly indicates the extremely low contrast of multi-spectral values in areas without visible vegetation.

The multi-spectral data were visualized and analyzed by using vegetation indices. In both datasets from August and November, the most significant contrast was displayed by the NDVI and the GEMI. The GNDVI is more sensitive to chlorophyll content and thus is mainly valuable for very green vegetation areas. The clear positive anomalies in the upper part of the north-eastern region are visible with the GNDVI, but the less green anomalies proved more challenging to detect with this index. The NDVI and GEMI indicated the same anomalies. The increased contrast of the GEMI dataset due to the limitation of atmospheric influences significantly enhanced the detection of cropmarks. In

the case of Voulokaliva, the GEMI vegetation index provided the best results in both the August and the November datasets. However, as hypothesized in chapters 2 and 4, the area's limited vegetation in August and November decreases the functionality of vegetation indices.

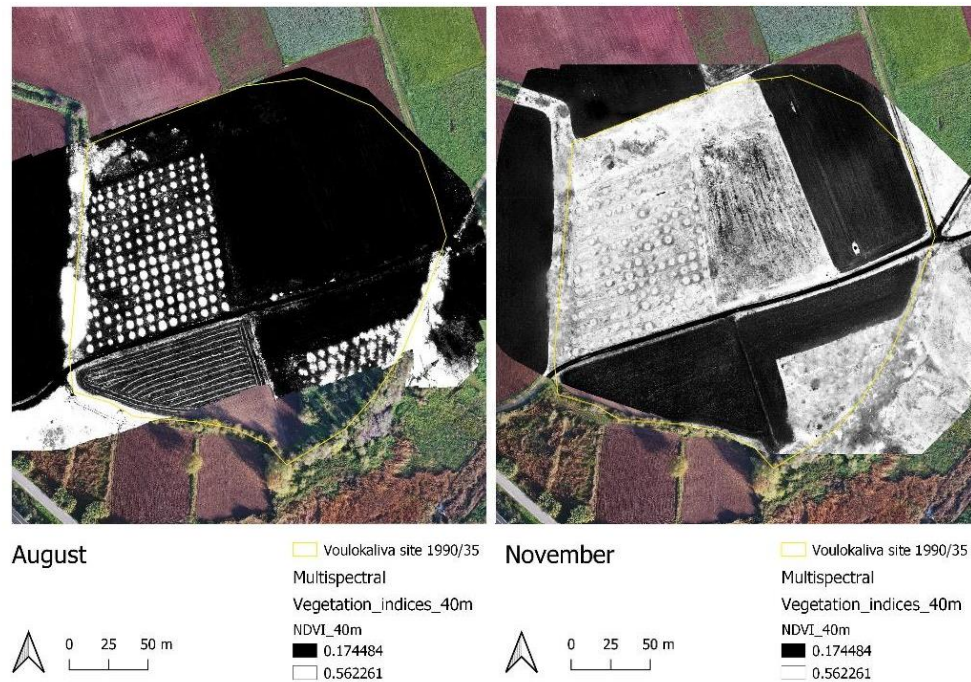


*Figure 19. Multi-spectral data collected in August (LEFT) and November (RIGHT) visualized with the NDVI*

### 6.1.2 Geophysical prospection

The geophysical prospection methods delivered a large number of potential archaeological features. The data was only collected at the western part of the site and mainly in the southwestern region. Thus, unfortunately, the anomalies detected by aerial imagery in the north-eastern part of the research area cannot be checked on the geophysical data.

Ground-penetrating radar revealed numerous archaeological remains in the southwestern part of the site and clear results appear on GPR depth slices to a depth of 160 centimeters. These results are surprising since the site's soil consists mainly of clay and clay particles are known to decrease ground-penetrating radar results significantly. The geomagnetic survey results showed increased noise in the dataset. However, still, a large number of anomalies were uncovered. Clay soils are not ideal for geomagnetic survey, but if the conditions are favorable, it might produce good results. The electromagnetic induction survey at this site illustrates the point made by Sarris and colleagues (2017). They argue that electromagnetic induction survey is best applied as a general prospection method, which can be used to select regions for more detailed investigation. At Voulokaliva site 1990/35, the electromagnetic induction survey showed interesting regions with low conductivity,

high viscosity and low susceptibility values. The earth resistance survey highlighted several areas of high resistance. The contrast between the soil matrix and potential features proves very high and anomalies are clearly visible. The large number of anomalies detected on the geophysical datasets show that even if the soil conditions are not ideal for this type of prospection, good results can still be achieved if the environmental conditions are favorable.

### 6.1.3 Comparative analysis

The comparative analysis proved difficult since the data collection of each remote sensing technique was restricted to particular areas; the results were thus highly influenced by the availability of data. A noticeable observation is a high correlation between geomagnetic survey and ground-penetrating radar results. Both techniques do not necessarily provide clear results in clay soils; however, these datasets show high contrasts and apparent anomalies. As mentioned by Armstrong & Kalayci, the Mediterranean climate provides favorable conditions for geomagnetic survey. Geomagnetic surveys can respond well to clay soils, if under the right climatic conditions. In the case of Voulokaliva, the Mediterranean climate and clay soil proved very suitable for geomagnetic survey. The GPR data also does not necessarily respond well to clay soils, especially if the soil is very wet. Whereas the dry spells in Thessaly might have decreased the thermal data, ground-penetrating radar responds better to dry soils. Both the geomagnetic survey as the ground penetrating radar have provided good results under the Mediterranean climate and soil conditions. Another remark involves the linear anomalies in the northwestern region. Geomagnetic survey, multi-spectral imagery and electromagnetic induction survey indicate ditch-like features. Besides thermography, no other techniques were applied in this area and the thermal data was affected by the olive trees. It is thus not clear whether other techniques would have uncovered these anomalies or whether they are restricted to geomagnetic survey, multi-spectral imagery and electromagnetic induction. To better understand the possibilities of remote sensing techniques at Voulokaliva, the different areas must be subjected to all techniques. However, the similarities and discrepancies between the datasets that overlap have already shown that no technique is able to uncover all archaeological features. The variation in local soil and vegetation conditions demonstrates the need to apply various remote sensing techniques.

### 6.2 Interpretation of the results

This section will discuss the possible interpretation of the results of both the individual datasets as the comparative analysis. For organizational purposes, the area is divided into four regions: northwestern, northeastern, southeastern, and southwestern.



The northwestern region was subjected to thermography, multi-spectral imagery, geomagnetic, and electromagnetic surveys. The aerial imagery uncovered little archaeological remains since the olive trees obstructed the view of the soil. In 2015, during the geophysical prospection, these trees were in a very early stage and did not pose a problem. The geomagnetic survey revealed two semi-circular anomalies which extend for 170 meters. The features are closely linked to the organization of the settlement, indicating ditches encircling the site. The location of the two potential ditches supports the hypothesis that the site was expanded later in time (see Sarris et al., 2016 and figure 6). The linear anomaly crossing these lines possibly indicates a corridor or roadway. The comparative analysis showed that the potential ditches correspond with the low conductivity and high viscosity anomalies detected on the electromagnetic induction survey data. In addition, the multi-spectral data revealed a semi-circular positive anomaly in the same location. This positive cropmark reinforces the hypothesis of ditches enclosing the site in this part of the research area. Furthermore, the geomagnetic data shows circular anomalies located in the upper part of this region, which might indicate small pits relating to the Late Neolithic and Early Bronze Age occupation of Voulokaliva (Sarris et al., 2016).

The northeastern part of the research area was only subjected to aerial imagery. The aforementioned circular anomalies detected on the geomagnetic data also appear on the northeastern region's multi-spectral data. The upper part of the northeastern area contains five positive circular anomalies, which can be interpreted as pit-like features. The nature of the multi-spectral features thus seems to correspond to the features found 13 meters to the West. The thermal data visualized two large anomalies in this region with temperatures lower than the surrounding soil matrix, which might indicate the presence of ditches. The anomalies are not visible on the optical data collected on the same day, which makes it less probable that the anomalies are, in fact, tractor traces. It is remarkable that both datasets uncover different pit-like features that are not visible on the other dataset. This could indicate that the pits are filled with different materials, which respond either to thermal or multi-spectral technologies. Excavational data and soil samples might be able to shed light on why the materials appear only on one of either datasets. Anomaly 3 does correspond with the angular multi-spectral anomaly 17. The angle, straight lines and negative cropmark indicate the presence of structural remains, whereas anomaly 3 suggests a pit-like feature. The very distinct results between the thermal and multi-spectral data within a relatively small area, show that even tiny differences in soil and feature conditions can impact the visibility of anomalies on remote sensing data.

In the southeastern region, too, only thermal and multi-spectral data were collected. No anomalies were discovered in this part of the research area.

The southwestern region produced the most results, which is directly related to the number of methods applied here. This area was exposed to thermography, multi-spectral imagery, ground-penetrating radar, geomagnetic, and soil resistance surveys. Ground-penetrating radar exposed two linear interrupted anomalies, corresponding to a linear anomaly discovered on the geomagnetic data. This linear feature is hypothesized to represent a gate or corridor, the strong reflectance of the other GPR anomalies indicates stone structures or foundations (Sarris et al., 2016). The soil resistance survey showed rectangular-shaped anomalies, possibly indicating structures and linear anomalies, suggesting stone-based foundations. A clear correlation consists of the ground-penetrating radar, geomagnetic survey and soil resistance survey, however, Sarris et al. (2016) mentions that the geomagnetic anomalies do not suggest architectural remains but only pit and ditch like features. This is remarkable since the size and direction of the ground-penetrating radar and soil resistance survey anomalies indicate a built environment with a high-density clustering of structures. This could suggest that geomagnetic techniques were not able to pinpoint structural remains under the conditions of Voulokaliva. A linear anomaly is visible in the western part of the region on both the geomagnetic survey data and the multi-spectral data. This anomaly seems to correspond to the outer ditch found in the northwestern part of the site. Noticeably, the southwestern area is mainly filled with linear anomalies indicating stone structures and no ditches or pits were distinguished. The geomagnetic data did locate some circular dipole anomalies, but their orientation suggests the presence of metal fragments (Sarris et al., 2016).

In general, a pattern can be distinguished between pit- and ditch-like features in the northern part of the research area and stone structures and foundations in the southern part of the area. The results from the archaeological surveys substantiate this differentiation. The survey showed that the materials found in the northern part of the site are linked to the Late Neolithic and Early Bronze Age, characterized by pits and ditches. The southern region was primarily occupied during the Late Bronze Age and Early Iron Age, in which structural remains became more common (H. Reinders, 2004).

Both the discovery of anomalies and the interpretation of the dataset are highly dependent on the researcher's knowledge, expertise and experience. The researcher's bias needs to be kept in mind when interpreting remote sensing results. Furthermore, it must be kept in mind that a lack of visible anomalies does not necessarily mean a lack of archaeological remains. The data collection is affected by environmental circumstances, pre-and postprocessing, and the quality and alignment of the instrument, among others.

### 6.3 Concluding remarks

This chapter aims to answer three sub-questions. The remote sensing approaches that proved most useful were ground-penetrating radar, geomagnetic survey and earth resistance survey. The comparative approach showed that ground-penetrating radar and earth resistance survey highlighted significantly different remains than the geomagnetic survey. Ground-penetrating radar and earth resistance survey revealed structural remains, whereas the geomagnetic survey only indicated ditch and pit-like features. This might indicate that the specific conditions at Voulokaliva made it difficult to discover structural remains on geomagnetic survey data, whereas pit-like features were easily detectable. The aerial imagery provided limited results due to environmental and vegetational conditions. However, the few results demonstrated that even in a relatively small area, the visibility of anomalies on remote sensing data can be highly affected by tiny differences in soil and feature conditions. The interpretation of the anomalies shows a significant correlation to the field survey results discussed by Stissi and colleagues (2015) and added valuable information on the distribution of archaeological features. These results demonstrate both the possibilities and the limitations of remote sensing applications in the discovery of archaeological remains.

## 7. Conclusion

### 7.1 Introduction

This thesis aimed to increase knowledge of the possibilities and limitations of remote sensing techniques when employed in archaeological prospection. A comparative approach is implemented to construct a consolidated overview of different remote sensing technologies. The theoretical framework was applied in the case study at Voulokaliva. The remote sensing results were examined in QGIS and exposed to different analysis and visualization methods. After the thermal and multi-spectral anomalies were identified, they were combined with the geophysical anomalies in a comparative analysis. The goal of this research was to answer the following question:

How do the different remote sensing techniques operate in visualizing potential archaeological remains at Voulokaliva, Halos, Greece (Late Neolithic to the Early Iron Age) and how can these findings aid in developing a more targeted approach to archaeological prospection?

This question was assessed by comparing aerial imagery and geophysical techniques applied at Voulokaliva. The results of the comparative analysis mainly highlighted the diverse effects of external factors on remote sensing applications. The aerial imagery produced limited results, which was highly influenced by agricultural practices and vegetation. In contrast, the geophysical results presented a surprisingly large number of anomalies, even though clay-rich soil is not ideal in most geophysical prospection applications.

The advantage of remote sensing as a component of archaeological prospection is demonstrated by a large number of discovered anomalies and their correspondence to previous survey results. The anomalies seem to be consistent with the archaeological expectation of the region, but they also provide a more detailed and specific image of feature distribution. The chronological division of the site is highlighted by the presence of Late Neolithic and Early Bronze Age pit-like features in the northern part of the research area, in contrast to Late Bronze Age structural remains in the southern region. These results substantiate the hypothesis put forward by Reinders (2004) and provide new knowledge on this site, which is crucial to the understanding of the Voulokaliva area.

This thesis showed the potential of using an integrative approach. Some anomalies appeared on multiple datasets, but many significant anomalies were only visible with one or two remote sensing techniques. A combination of different remote sensing applications is necessary to create a comprehensive view of the potential archaeological remains at a site. However, this research also highlighted the importance of prior knowledge of external factors in the research area, both of the general site conditions and of variations within the site itself. The environment, soil conditions,

archaeological materials and other influences should be assessed beforehand to construct a site-specific remote sensing toolbox. The preliminary analysis can enhance the quality of remote sensing data and limit the amount of unusable data due to external factors, which could lead to a significant decrease in time and money spent.

## 7.2 Future research

The countless possibilities of remote sensing techniques in discovering archaeological remains are widely renowned. However, the limitations are not yet fully explored. This research aims at implementing a theoretical approach to remote sensing techniques within archaeological prospection. This framework can be built upon by future research to provide a more comprehensive view of the use of remote sensing in mapping archaeological remains.

First it is important to acknowledge that the remote sensing techniques applied in this thesis are not yet investigated with more invasive techniques. Excavating the research area can be used to ground-truth the anomalies and discover which anomalies indicate actual archaeological features. Also it can shed light on features that did not appear on the remote sensing data and the materials they are made of.

This research provided insights into the possibilities and limitations of remote sensing applications in the field of archaeological prospection. Voulokaliva was subjected to many remote sensing techniques; however, the different techniques were not applied to the entire research area, which complicated the comparative analysis. When looking at Voulokaliva individually, future research might aim at applying the aforementioned remote sensing techniques to the complete site. This would provide a more comprehensive dataset for comparative analysis and shed light on the potential of different remote sensing techniques under these specific conditions. Also, this site might then be used as an example for other comparable Mediterranean archaeological sites. More extensive research can also focus on applying the remote sensing techniques at Voulokaliva under varying conditions. These conditions can consist of different seasons, weather circumstances or time frames. The Sentinel-2 data from April, for instance, showed much vegetation, which might provide better multi-spectral results. By these means, the ideal circumstances for each dataset can be further investigated. This research can also be extended to other climate zones, periods, soil conditions and varying archaeological materials. The ideal outcome would be a comprehensive database on the possibilities and limitations of all remote sensing techniques under different circumstances and environmental conditions.

Furthermore, additional research can be applied to discover the possibilities of multi-spectral imagery. In the case of Voulokaliva, the multi-spectral data delivered minimal results due to insufficient vegetation. Another possibility would be the application of soil indices, which are focused more on soil data and are less impacted by vegetation. Soil indices often make use of data captured on the SWIR bands, which was not available for this thesis. Future research can aim to collect data at different wavelengths (Aqdus et al., 2012).

Finally, this thesis makes use of a comparative approach between individual datasets. The data is visually scanned for anomalies and compared in isolation. A statistical or mathematical integration of the remote sensing data can be applied to combine the individual datasets into one. The integration of the datasets can be used to make a single interpretation of potential anomalies. Also, this thesis utilizes visual detection of anomalies. Aqdus and colleagues (2012) propose to bridge the gap between aerial archaeologists and remote sensing specialists. Remote sensing specialists often use filters and mathematical algorithms to quantify image analysis, whereas aerial archaeologists often rely on visual detection. A possibility is the automatization of anomaly detection, for example with machine-learning methods or different image processing techniques. The detection and comparison of remote sensing anomalies is very time consuming and statistical methods can significantly reduce time spent.

Though more extensive research is required, this thesis facilitates a richer understanding of remote sensing techniques in general and applied at Voulokaliva. This can support future remote sensing operators in deciding which technique should be employed under conditions similar to Voulokaliva, or the Mediterranean environment. This research takes a step towards the application of site characteristics to a selection of remote sensing techniques and the foundation of a consolidated database on remote sensing technologies.

## Abstract

Remote sensing is widely applied within archaeological prospection. Numerous scientific studies have demonstrated the potential of remote sensing techniques in discovering archaeological remains. However, remote sensing data is influenced by external factors, such as climate, vegetation and moisture content. Not every remote sensing application is sensitive to each variable and detected anomalies can vary significantly between datasets. The latest trend involves the integration of remote sensing data to limit the possibility that archaeological features remain uncovered. An assessment of these external factors can be used to apply more targeted research at potential archaeological sites. Current prospection methods occasionally deliver poor results and a better understanding of external factors could lead to a significant decrease in time and money.

This research aims at constructing a consolidated overview of two aerial imagery and four geophysical prospection techniques, their applicability in archaeological prospection and the ideal conditions to collect their respective datasets. The different techniques, namely thermography, multi-spectral imagery, ground-penetrating radar, geomagnetic survey, electromagnetic induction survey and earth resistance survey, are subjected to a comparative approach executed in the open-source application QGIS.

A large number of anomalies were discovered and the best results were obtained with ground-penetrating radar, geomagnetic survey and earth resistance survey. The aerial imagery did not produce many results, which can be attributed to environmental and vegetation circumstances. The results essentially correspond with the findings of previous fieldwalking surveys. Nevertheless, the remote sensing techniques provided interesting insights into feature distribution patterns and the location of structural remains.

This thesis provides a framework to assess the possibilities and limitations of remote sensing within archaeological prospection and shows the potential of using an integrative approach. However, this assessment also illustrates the research gap between the theoretical and practical application of remote sensing techniques within the archaeological field.

## Bibliography

- Agapiou, A., Alexakis, D. D., Sarris, A., & Hadjimitsis, D. G. (2013). Orthogonal Equations of Multi-Spectral Satellite Imagery for the Identification of Un-Excavated Archaeological Sites. *Remote Sensing*, 5(12), 6560–6586. <https://doi.org/10.3390/rs5126560>
- Agapiou, A., & Lysandrou, V. (2015). Remote sensing archaeology: Tracking and mapping evolution in European scientific literature from 1999 to 2015. *Journal of Archaeological Science: Reports*, 4, 192–200. <https://doi.org/10.1016/j.jasrep.2015.09.010>
- Agudo, P. U., Pajas, J. A., Pérez-Cabello, F., Redón, J. V., & Lebrón, B. E. (2018). The Potential of Drones and Sensors to Enhance Detection of Archaeological Cropmarks: A Comparative Study Between Multi-Spectral and Thermal Imagery. *Drones*, 2(3), 29. <https://doi.org/10.3390/drones2030029>
- Annan, P. (2009). Chapter 1. Electromagnetic Principles of Ground Penetrating Radar. In *Ground Penetrating Radar: Theory and Applications* (pp. 1–40). <https://doi.org/10.1016/B978-0-444-53348-7.00001-6>
- Aqdas, S. A., Hanson, W. S., & Drummond, J. (2012). The potential of hyperspectral and multi-spectral imagery to enhance archaeological cropmark detection: A comparative study. *Journal of Archaeological Science*, 39(7), 1915–1924. <https://doi.org/10.1016/j.jas.2012.01.034>
- Armstrong, K. L., & Kalayci, T. (2015). Images of the Past: Magnetic Prospection in Archaeology. In A. Sarris (Ed.), *Best Practices of Geoinformatic Technologies for the Mapping of Archaeolandscapes*. Archaeopress Archaeology.
- Baroň, I., Bečkovský, D., & Mica, L. (2013). Application of infrared thermography for mapping open fractures in deep-seated rockslides and unstable cliffs. *Landslides*, 11. <https://doi.org/10.1007/s10346-012-0367-z>
- Campana, D. S. (2016). *Archaeology, Remote Sensing*. 703–724.
- Casana, J., Wiewel, A., Cool, A., Hill, A. C., Fisher, K. D., & Laugier, E. J. (2017). Archaeological Aerial Thermography in Theory and Practice. *Advances in Archaeological Practice*, 5(4), 310–327. <https://doi.org/10.1017/aap.2017.23>
- Christmann, E., & Karimali, E. (2004). Late Neolithic and Early Bronze Age. In H. R. Reinders (Ed.), *Prehistoric Sites at the Almirós and Sóurpi Plains (Thessaly, Greece)*. Uitgeverij Van Gorcum.
- Congedo, L. (2021). Semi-Automatic Classification Plugin: A Python tool for the download and processing of remote sensing images in QGIS. *Journal of Open Source Software*, 6(64), 3172. <https://doi.org/10.21105/joss.03172>



- Cool, A. C. (2018). Thermography. *The Encyclopedia of Archaeological Sciences*.  
<https://www.academia.edu/30448375/Thermography>
- Doolittle, J. A., & Butnor, J. R. (2009). Soils, Peatlands, and Biomonitoring. In H. M. Jol (Ed.), *Ground Penetrating Radar: Theory and Applications: Vol. 1st ed.* Elsevier Science.
- El-Qady, G., Metwaly, M., & Drahor, M. G. (2018). Geophysical Techniques Applied in Archaeology. In G. El-Qady & M. Metwaly (Eds.), *Archaeogeophysics: State of the Art and Case Studies*. Springer International Publishing AG.
- Floras, S., & Sgouras, I. (2004). The Almirós and Soúрпи Plains. In H. R. Reinders (Ed.), *Prehistoric Sites at the Almirós and Soúрпи Plains (Thessaly, Greece)*. Uitgeverij Van Gorcum.
- Gaffney, C. (2008). Detecting Trends in the Prediction of the Buried Past: A Review of Geophysical Techniques in Archaeology\*. *Archaeometry*, 50(2), 313–336. <https://doi.org/10.1111/j.1475-4754.2008.00388.x>
- Huete, A. R. (1988). A soil-adjusted vegetation index (SAVI). *Remote Sensing of Environment*, 25(3), 295–309. [https://doi.org/10.1016/0034-4257\(88\)90106-X](https://doi.org/10.1016/0034-4257(88)90106-X)
- Jensen, J. R. (2014). *Remote Sensing of the Environment: An Earth Resource Perspective*. Pearson Prentice Hall.
- Karouzou, E. (2019). Thessaly. In *A Companion to the Archaeology of Early Greece and the Mediterranean* (Vol. 2). John Wiley & Sons.  
<https://onlinelibrary.wiley.com/doi/10.1002/9781118769966.ch36>
- Kokalj, Ž., & Hesse, R. (2017). *Airborne laser scanning raster data visualization*.  
<https://doi.org/10.3986/9789612549848>
- Kokalj, Ž., & Somrak, M. (2019). Why Not a Single Image? Combining Visualizations to Facilitate Fieldwork and On-Screen Mapping. *Remote Sensing*, 11, 747.  
<https://doi.org/10.3390/rs11070747>
- Lagia, A., Papathanasiou, A., Malakasioti, Z., & Tsiouka, F. (2013). *Cremations of the Early Iron Age from Mound 36 at Voulokalyva (Ancient Halos) in Thessaly: A Bioarchaeological Appraisal* (pp. 192–214).
- Loukas, A., Vasiliades, L., & Tzabiras, J. (2008). Climate change effects on drought severity. *Advances in Geosciences*, 17, 23–29. <https://doi.org/10.5194/adgeo-17-23-2008>
- Manataki, M., Sarris, A., Donati, J. C., Garcia, C. C., & Kalayci, T. (2015). GPR: Theory and Practice in Archaeological Prospection. In A. Sarris (Ed.), *Best Practices of Geoinformatic Technologies for the Mapping of Archaeolandscapes*. Archaeopress Archaeology.
- Materazzi, F., & Pacifici, M. (2022). Archaeological crop marks detection through drone multispectral remote sensing and vegetation indices: A new approach tested on the Italian pre-Roman city

- of Veii. *Journal of Archaeological Science: Reports*, 41, 103235.  
<https://doi.org/10.1016/j.jasrep.2021.103235>
- Moffat, I. (2015). Locating Graves with Geophysics. In A. Sarris (Ed.), *Best Practices of Geoinformatic Technologies for The Mapping of Archaeolandscapes*. Archaeopress Archaeology.
- Nathalie Pettorelli. (2013). *The Normalized Difference Vegetation Index*. OUP Oxford.  
<https://login.ezproxy.leidenuniv.nl:2443/login?URL=https://search.ebscohost.com/login.aspx?direct=true&db=e000xww&AN=650477&site=ehost-live>
- Pappalardo, G., Mineo, S., Angrisani, A. C., Di Martire, D., & Calcaterra, D. (2018). Combining field data with infrared thermography and DInSAR surveys to evaluate the activity of landslides: The case study of Randazzo Landslide (NE Sicily). *Landslides*, 15(11), 2173–2193.  
<https://doi.org/10.1007/s10346-018-1026-9>
- Périsset, M., & Tabbagh, A. (1981). Interpretation of thermal prospection on bare soils. *Archaeometry*, 23, 169–187. <https://doi.org/10.1111/j.1475-4754.1981.tb00304.x>
- Pinty, B., & Verstraete, M. M. (1992). GEMI: A non-linear index to monitor global vegetation from satellites. *Vegetatio*, 101(1), 15–20. <https://doi.org/10.1007/BF00031911>
- Reinders, H. (2004). *Prehistoric Sites at the Almirós and Sóurpi Plains (Thessaly, Greece)*. Uitgeverij Van Gorcum.
- Rodrigues, S. I., Porsani, J. L., Santos, V. R. N., DeBlasis, P. A. D., & Giannini, P. C. F. (2009). GPR and inductive electromagnetic surveys applied in three coastal sambaqui (shell mounds) archaeological sites in Santa Catarina state, South Brazil. *Journal of Archaeological Science*, 36(10), 2081–2088. <https://doi.org/10.1016/j.jas.2009.05.013>
- Rondeaux, G., Steven, M., & Baret, F. (1996). Optimization of soil-adjusted vegetation indices. *Remote Sensing of Environment*, 55(2), 95–107. [https://doi.org/10.1016/0034-4257\(95\)00186-7](https://doi.org/10.1016/0034-4257(95)00186-7)
- Saleh, B. E. A. (2011). *Introduction to Subsurface Imaging*. Cambridge University Press.
- Sarris, A. (2017). Geophysics. In A. S. Gilbert (Ed.), *Encyclopedia of Geoarchaeology* (pp. 323–326). Springer Netherlands. [https://doi.org/10.1007/978-1-4020-4409-0\\_166](https://doi.org/10.1007/978-1-4020-4409-0_166)
- Sarris, A., Kalayci, T., Moffat, I., Donati, J., Manataki, M., Argyrioy, N., Cantoro, N. N. G., & Efstathiou, S. (2016). *Technical report on geophysical survey at Voulokaliva (site 1990/35)* (Technical Report MIS-448300; pp. 1–13). GeoSat ReSeArch Lab, Institute for Mediterranean Studies, Foundation for Research and Technology Hellas (IMS/FORTH).
- Sarris, A., Kalayci, T., Moffat, I., & Manataki, M. (2017). An Introduction to Geophysical and Geochemical Methods in Digital Geoarchaeology. In C. Siart, M. Forbriger, & O. Bubbenzer (Eds.), *Digital Geoarchaeology: New Techniques for Interdisciplinary Human-Environment Research*. Springer International Publishing AG.

- Sarris, A., Papadopoulos, N., Agapiou, A., Salvi, M. C., Hadjimitsis, D., Parkinson, W., Yerkes, R., Gyucha, A., & Duffy, P. R. (2013). Integration of geophysical surveys, ground hyperspectral measurements, aerial and satellite imagery for archaeological prospection of prehistoric sites: The case study of Vészto{doubleacute}-Mágor Tell, Hungary. *Journal of Archaeological Science*, *40*, 1454–1470. <https://doi.org/10.1016/j.jas.2012.11.001>
- Schmidt, A. (2013). *Earth resistance for archaeology* (Vol. 3). AltaMira Press.
- Simon, F.-X., Kalayci, T., Donati, J. C., Cuenca Garcia, C., Manataki, M., & Sarris, A. (2015). How efficient is an integrative approach in archaeological geophysics? Comparative case studies from Neolithic settlements in Thessaly (Central Greece). *Near Surface Geophysics*, *13*(6), 633–643. <https://doi.org/10.3997/1873-0604.2015041>
- Simon, F.-X., Tabbagh, A., Julien, T., & Sarris, A. (2015). Mapping of quadrature magnetic susceptibility/magnetic viscosity of soils by using multi-frequency EMI. *Journal of Applied Geophysics*, *120*, 36–47. <https://doi.org/10.1016/j.jappgeo.2015.06.007>
- Stissi, V. (2004). Late Bronze Age. In H. R. Reinders (Ed.), *Prehistoric Sites at the Almirós and Soúrpi Plains (Thessaly, Greece)*. Uitgeverij Van Gorcum.
- Stissi, V., Kwak, L., & de Winter, J. (2004). Early Iron Age. In H. R. Reinders (Ed.), *Prehistoric Sites at the Almirós and Soúrpi Plains (Thessaly, Greece)*. Uitgeverij Van Gorcum.
- Stissi, V., Waagen, J., Reinders, R., Rondiri, V., Mamaloudi, I., Stamelou, E., & Rousseau, A. (2015). *Halos: Preliminary report of the 2011-2013 field survey campaigns*. 63–84. <https://doi.org/10.2143/PHA.21.2.3206295>
- Tang, P., Chen, F., Jiang, A., Zhou, W., Wang, H., Leucci, G., de Giorgi, L., Sileo, M., Luo, R., Lasaponara, R., & Masini, N. (2018). Multi-frequency Electromagnetic Induction Survey for Archaeological Prospection: Approach and Results in Han Hangu Pass and Xishan Yang in China. *Surveys in Geophysics*, *39*(6), 1285–1302. <https://doi.org/10.1007/s10712-018-9471-5>
- Tapete, D. (2018). Remote Sensing and Geosciences for Archaeology. *Geosciences*, *8*(2), 41. <https://doi.org/10.3390/geosciences8020041>
- Themistocleous, K., Agapiou, A., Cuca, B., & Hadjimitsis, D. G. (2015). *Unmanned aerial systems and spectroscopy for remote sensing applications in archaeology*. <https://ktisis.cut.ac.cy/handle/10488/9392>
- Themistocleous, K., Hadjimitsis, D., Agapiou, A., Alexakis, D., & Sarris, A. (2013). *Remote Sensing for Archaeological Applications: Management, Documentation and Monitoring*. <https://doi.org/10.5772/39306>
- Verhoeven, G. (2017). *The reflection of two fields – Electromagnetic radiation and its role in (aerial) imaging*. *55*, 13–18. <https://doi.org/10.5281/zenodo.3534245>

Walker, S. (2020). Low-altitude aerial thermography for the archaeological investigation of arctic landscapes. *Journal of Archaeological Science*, 117, 105126.

<https://doi.org/10.1016/j.jas.2020.105126>

Zheng, W., Li, X., Lam, N., Wang, X., Liu, S., Yu, X., Sun, Z., & Yao, J. (2013). Applications of integrated geophysical method in archaeological surveys of the ancient Shu ruins. *Journal of Archaeological Science*, 40(1), 166–175. <https://doi.org/10.1016/j.jas.2012.08.022>

## List of figures

Figure 1. Sentinel-2 RGB data of Voulokaliva site 1990/35 in April, August and November 2021.....	12
Figure 2. Map of the fieldwalking survey in 2011-2013 depicting the find collection grids and field numbers by Jitte Waagen (Stissi et al., 2015).....	14
Figure 3: Schematic representation of the working principle of thermography.....	18
Figure 4. Schematic representation of cropmarks caused by anthropological features.....	21
Figure 5. The working principle of Ground Penetrating Radar.....	23
Figure 6. A schematic representation of geomagnetic survey.....	24
Figure 7. A representation of the electromagnetic induction principle.....	25
Figure 8. A schematic representation of earth resistance survey.....	27
Figure 9. The thermography results of Voulokaliva site 1990/35, positioned on the thermal and optical data collected in August.....	34
Figure 10. The multi-spectral imagery results of Voulokaliva site 1990/35, superimposed on the multi-spectral data collected in November (GEMI vegetation index).....	35
Figure 11. The multi-spectral imagery results of Voulokaliva site 1990/35, superimposed on the multi-spectral data collected in November (NDVI vegetation index).....	35
Figure 12. The multi-spectral imagery results of Voulokaliva site 1990/35, superimposed on the multi-spectral data collected in August (GEMI vegetation index).....	36
Figure 13. The multi-spectral imagery results of Voulokaliva site 1990/35, superimposed on the multi-spectral data collected in August (NDVI vegetation index).....	36

Figure 14. The ground-penetrating radar results of Voulokaliva site 1990/35, positioned on the optical data collected at the height of 250 meters (after Sarris et al., 2016).....	37
Figure 15. The geomagnetic survey results of Voulokaliva site 1990/35, superimposed on the optical data collected at the height of 250 meters (after Sarris et al., 2016).....	38
Figure 16. The electromagnetic induction survey results of Voulokaliva site 1990/35, positioned on the optical data collected at the height of 250 meters. From left to right: conductivity, viscosity and susceptibility at the frequency of 43350 Hz (TOP) and the interpretation of the anomalies (BOTTOM) (after Sarris et al., 2016).....	39
Figure 17. The earth resistance survey results of Voulokaliva site 1990/3, overlaid on the optical data collected at the height of 250 meters (after Sarris et al., 2016).....	40
Figure 18. Comparison of all discovered anomalies superimposed on the optical dataset collected at the height of 250 meters.....	42
Figure 19. Multi-spectral data collected in August (LEFT) and November (RIGHT) visualized with the NDVI vegetation index.....	46

## List of tables

Table 1. The division of optical electromagnetic radiation based on wavelength and the imaging principle (after Verhoeven, 2017).....	17
Table 2. Overview of suitable and unsuitable conditions for geomagnetic survey (Armstrong & Kalayci, 2015).....	25
Table 3. An overview of the vegetation indices that are used in this research.....	31-32
Table 4. An overview of the anomalies on multiple datasets and their respective length in meters, the numbers can be read as: <i>anomaly_number [length in meters]</i> .....	41-42

# List of appendices

Appendix I: Overview of the details and environmental conditions

of the drone flights by Waagen to collect thermal, multi-spectral and optical data of Voulokaliva site  
1990/35.....62-64

Appendix II: Overview of the details of the geophysical prospection by Sarris at Voulokaliva site

1990/35.....65-66

## Appendix I

Overview of the details and environmental conditions of the drone flights by Waagen to collect thermal, multi-spectral and optical data of Voulokaliva site 1990/35

<b>Dataset</b>	Thermal, 40m, site 35_transparent_reflectance_grayscale_1_1	Thermal, 80m, site 35_noalpha_reflectance_grayscale	Multi_40m_site35_transparent_reflectance_blue	Multi_40m_site35_transparent_reflectance_green	Multi_40m_site35_transparent_reflectance_nir
<b>Data Type</b>	Thermal	Thermal	Multispectral	Multispectral	Multispectral
<b>Spectral Band</b>	Infrared	Infrared	Blue	Green	Near Infrared
<b>Flight Date</b>	25 <sup>th</sup> of August 2021	25 <sup>th</sup> of August 2021	25 <sup>th</sup> of August 2021	25 <sup>th</sup> of August 2021	25 <sup>th</sup> of August 2021
<b>Flight Time</b>	After Sunset (21.15)	After Sunset (20.30)	Mid-Day (12.30/13.00)	Mid-Day (12.30/13.00)	Mid-Day (12.30/13.00)
<b>Drone Type</b>	M210 XT2	M210 XT2	M210 Micasense	M210 Micasense	M210 Micasense
<b>Altitude</b>	40m	80m	40m	40m	40m
<b>Current temperature</b>	27.0	28.5	34.9/33.6	34.9/33.6	34.9/33.6
<b>Maximum temperature</b>	35.0	35.0	35.0	35.0	35.0
<b>Minimum temperature</b>	23.0	23.0	23.0	23.0	23.0
<b>Light conditions</b>	After dusk	After dusk	Clear	Clear	Clear
<b>Relative humidity</b>	52.2	51.4	32.5/32.6	32.5/32.6	32.5/32.6
<b>Moisture conditions</b>	Dry	Dry	Dry	Dry	Dry
<b>Vegetation type</b>	Wheat, olives, clover	Wheat, olives, clover	Wheat, olives, clover	Wheat, olives, clover	Wheat, olives, clover
<b>Superficial layer</b>	Sandy clay soil	Sandy clay soil	Sandy clay soil	Sandy clay soil	Sandy clay soil
<b>Soil matrix</b>	Clay	Clay	Clay	Clay	Clay

Multi_40m_site35_transparent_reflectance_red_edge	Multi_40m_site35_transparent_reflectance_red	Optical_VK_50m_site_35_up1	Optical_VK_50m_site_35_dsm	Multi_80m_VK_site35_in dex_blue	Multi_80m_VK_site35_in dex_green
Multispectral	Multispectral	Optical	DSM	Multispectral	Multispectral
Red Edge	Red	Optical	Optical	Blue	Green
25 <sup>th</sup> of August 2021	25 <sup>th</sup> of August 2021	August 2021	August 2021	25 <sup>th</sup> of November 2021	25 <sup>th</sup> of November 2021
Mid-Day (12.30)	Mid-Day	-	-	Mid-Day	Mid-Day
M210 Micasense	M210 Micasense	P4	P4	M210 Rededge	M210 Rededge
40m	40m	50m	50m	80m	80m
34.9/33.6	34.9/33.6	-	-	16.8	16.8
35.0	35.0	-	-	-	-
23.0	23.0	-	-	-	-
Clear	Clear	-	-	Sky has opened more fully	Sky has opened more fully
32.5/32.6	32.5/32.6	-	-	55.0	55.0
Dry	Dry	-	-	Dry since the night	Dry since the night
Wheat, olives, clover	Wheat, olives, clover	-	-	-	-
Sandy clay soil	Sandy clay soil	Sandy clay soil	Sandy clay soil	Sandy clay soil	Sandy clay soil
Clay	Clay	Clay	Clay	Clay	Clay



Multi_80m_VK_site35_in dex_nir	Multi_80m_VK_site35_ index_red_edge	Multi_80m_VK_site35_in dex_red	Optical_250m_VK_tran sparent_mosaic_group 1	Optical_250m_VK_dsm
Multispectral	Multispectral	Multispectral	Optical	DSM
Near Infrared	Red Edge	Red	Optical	Optical
25 <sup>th</sup> of November 2021	25 <sup>th</sup> of November 2021	25 <sup>th</sup> of November 2021	27 <sup>th</sup> of November 2021	27 <sup>th</sup> of November 2021
Mid-Day	Mid-Day	Mid-Day	Mid-Day	Mid-Day
M210 Rededge	M210 Rededge	M210 Red edge	P4	P4
80m	80m	80m	250m	250m
16.8	16.8	16.8	12.6	12.6
-	-	-	-	-
-	-	-	-	-
Sky has opened more fully	Sky has opened more fully	Sky has opened more fully	Sunny morning, few clouds	Sunny morning, few clouds
55.0	55.0	55.0	80.0	80.0
Dry since the night	Dry since the night	Dry since the night	-	-
-	-	-	-	-
Sandy clay soil	Sandy clay soil	Sandy clay soil	Sandy clay soil	Sandy clay soil
Clay	Clay	Clay	Clay	Clay

## Appendix II

Overview of the details of the geophysical prospection by Sarris at Voulokaliva site 1990/35

<b>Dataset</b>	Orthophoto_VK_site3 5	Magnetics_Line	Magnetics_Polygon	Conductivity_Polygon _High	Conductivity_Polygon _Low	Viscosity43350_Polygo n_High
<b>Survey Type</b>	Remotely Piloted Aerial System (RPAS)	Geomagnetic Survey	Geomagnetic Survey	Electromagnetic Induction Survey (EMI)	Electromagnetic Induction Survey (EMI)	Electromagnetic Induction Survey (EMI)
<b>Data Type</b>	Orthophoto	Magnetics	Magnetics	Conductivity	Conductivity	Viscosity
<b>Date</b>	16 <sup>th</sup> of April 2015	16 <sup>th</sup> of April 2015	16 <sup>th</sup> of April 2015	16 <sup>th</sup> of April 2015	16 <sup>th</sup> of April 2015	16 <sup>th</sup> of April 2015
<b>Instrument</b>	-	Multi-sensor gradiometry system	Multi-sensor gradiometry system	Geophex GEM-2	Geophex GEM-2	Geophex GEM-2
<b>Frequency</b>	-	-	-	43350 Hz	43350 Hz	43350 Hz
<b>Area covered</b>	10.27 ha	1.53 ha	1.53 ha	1.09 ha	1.09 ha	1.09 ha

Susceptibility43350_Polygon_High	GPR_Line_MediumDepth GPR_MediumDepth	Resistivity_Polygon_High
Electromagnetic Induction Survey (EMI)	Ground Penetrating Radar Survey (GPR)	Soil Resistance Survey
Susceptibility	GPR data	Soil resistance data
16 <sup>th</sup> of April 2015	16 <sup>th</sup> of April 2015	16 <sup>th</sup> of April 2015
Geophex GEM-2	Noggin smart cart plus	Twin probe
43350 Hz	250 MHz	-
1.09 ha	0.43 ha	0.28 ha